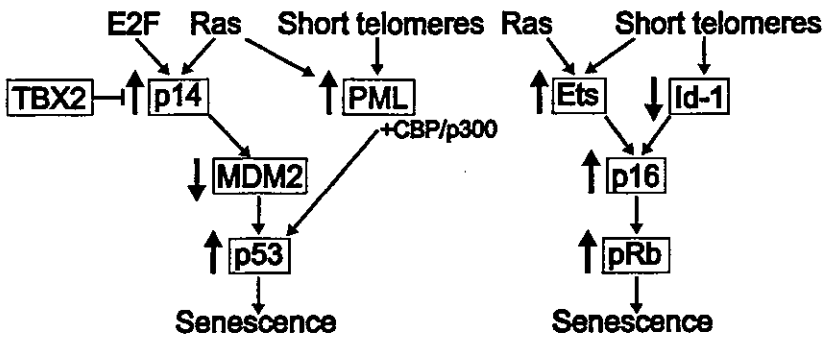

Fig. 3. Control of cellular senescence by the p53/p21 and p16/pRb pathways. Shown are the consequences of senescence-inducing signals on cell cycle regulators in the p53/p21 and p16/pRb pathways. Senescence-inducing signals, such as oncogenic Ras and E2F, increase expression of p14, whereas TBX2 represses p14 promoter activity, thus counteracting with each other. p14 sequesters MDM2, leading to an increase in p53 activity. Signals, such as oncogenic Ras, telomere shortening and possibly other signals increase expression of PML, which interacts with CBP/p300 and stimulates p53 activity. Oncogenic Ras stimulates the activity of Ets that induces p16 transcription by promoting its phosphorylation. Short telomeres lead to an increase in Ets and a decrease in Id, a protein that inhibits Ets activity, resulting in the accumulation of p16. p16 inhibits the cyclin-dependent kinases that phosphorylate pRb, leading to an increase in its active form.

promyelocytic leukemia (PML) tumor suppressor. PML is induced by replicative senescence and Ras activation by unknown mechanisms [72,73]. PML interacts with CBP/p300 acetyltransferase, which acetylates p53, thus stimulating p53 activity. Recently, p53 is found at telomeres and ablation of p53 function restores adverse effects of telomere loss [74], suggesting active roles of p53 in telomere maintenance as well as the telomere-response pathway. pRb exists in hypophosphorylated form that binds to E2F and inhibits cell cycle progression in senescent cells because of high levels of the cyclin-dependent kinase inhibitors, p21 and p16. p21 is transcriptionally induced at least partly by p53, although p53-independent, post-transcriptional mechanisms also contribute to an increase in p21 expression in senescent cells [75]. p16, another tumor-suppressor protein encoded by INK4a locus, increases in part because Ets, a transcription factor that stimulates p16 expression, is induced by senescent signals including telomere shortening and Ras activation, whereas Id1, a protein that inhibits Ets activity, is decreased in senescent cells [76]. It is demonstrated that ectopic expression of the cyclin-dependent kinase inhibitors, such as p21, p16 and p14, causes premature senescence [77], suggesting pivotal roles in the signaling pathways of senescence.

p53 immunoreactivity is present in vascular cells in areas with chronic inflammation of human atheroma, while a few cells positive for p53 immunoreactivity are found in control arteries [78]. p21 immunoreactivity is also detected in human atheroma but not in normal lesions and is colocalized with p53. Forced expression of cyclin-dependent kinase inhibitors induces premature senescence that is associated with cell dysfunction in cultured vascular cells (Minamino et al. unpublished data). These observations suggest a pathological role of p53 and p21 in atherogenesis. However, their precise roles remain unclear. It is demonstrated that atherosclerosis is aggravated in p53/apolipoprotein E (ApoE) double-knockout mice through an increase in p53-controlled proliferation [79]. In contrast, the study using perivascular collar model in ApoE-knockout mice shows that p53 overexpression results in a marked decrease in the cellular and extracellular contents in the cap lesions, leading to spontaneous plaque rupture [80]. Thus, in the clinical settings, elevated expression of p53 and cyclin-dependent kinase inhibitors may be deleterious in human atherosclerosis.

9. Ras-induced senescence and vascular inflammation

It has been demonstrated that various molecules including growth factors, vasoactive peptides and oxidative stresses, such as ROS and oxidized low-density lipoproteins, are induced during the lesion formation and regulate numerous critical cell functions, thereby contributing to atherogenesis [81]. These stimuli function as mitogens for vascular cells through the signaling cascades that activate Ras [81]. Inhibition of Ras has been reported to prevent intimal formation after vascular injury, suggesting a critical role of Ras activation in VSMC proliferation [82]. In addition to its role in cell proliferation, we have found that constitutive activation of Ras induces vascular cell senescence that is associated with vascular inflammation [20]. Activation of Ras drastically increased expression of pro-inflammatory cytokines partially through ERK activation in cultured vascular cells. Introduction of Ras into balloon-injured arteries enhanced vascular inflammation as well as senescence compared with control-injured arteries (Fig. 4). Moreover, senescent cells express inflammatory molecules in human atherosclerotic plaque, and ERK is activated in these cells, suggesting that telomere-independent mechanisms may also contribute to vascular cell senescence in human atherosclerosis. Consistent with our findings, functional inhibition of Ras has been demonstrated to suppress pro-inflammatory molecules, thereby reducing lesion formation in ApoE-deficient mice [83]. Moreover, angiotensin II, an important atherogenic molecule that activates the Ras-signaling pathway, has been demonstrated to promote vascular cell senescence as well as vascular inflammation [84]. Thus, it is assumed that atherogenic stimuli may

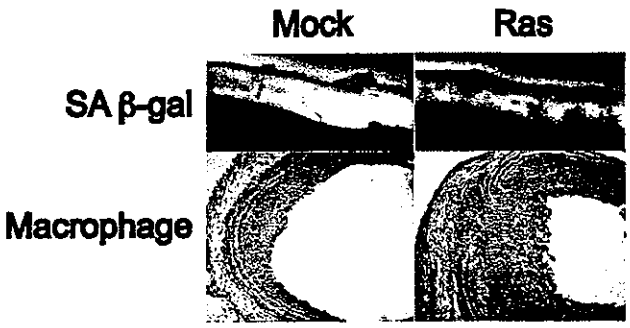

Fig. 4. Activation of Ras induces senescence and inflammation in vivo. The adenoviral vector encoding H-*ras*V12 (Ras) or the empty vector (Mock) was transduced into rat carotid arteries injured by a balloon catheter. It is known that accumulation of macrophages is minimally involved in the lesion formation in this model. Whereas only a little SA β-gal activity was found in mock-infected injured arteries, transduction of adeno-Ras into injured arteries increased SA β-gal activity (upper panel). The area of accumulated macrophages (brown) in the intima was markedly increased in Ras-infected injured arteries compared with mock-infected injured arteries (lower panel), indicating a causal relationship between Ras activation and vascular inflammation. Adapted from Ref. [20] with permission.

initially promote cell proliferation, and when overstimulated to proliferate, mitogenic-signaling pathways may induce telomere-dependent and telomere-independent senescence, which results in vascular dysfunction. Vascular inflammation is known to induce degradation of extracellular matrix by various proteinases, such as collagenases and gelatinases, and by inhibition of matrix production [85]. Therefore, decreased cellularity and enhanced inflammation associated with vascular cell senescence may contribute to plaque vulnerability.

10. Genetic models for aging

Many molecular mechanisms have been suggested to contribute to human aging and age-associated disease. Recent genetic analyses have demonstrated that reduction-of-function mutations of the signaling pathway of insulin/insulin-like growth factor-1 (IGF-1)/phosphatidylinositol-3 kinase (PI3K)/Akt (also known as protein kinase B) extends the longevity of the nematode *Caenorhabditis elegans* [86–92]. The forkhead transcription factor DAF-16, which is phosphorylated and thereby inactivated by Akt, plays an essential role in this longevity pathway [93,94]. More recently, it has been reported that the genes regulating longevity are conserved in organisms ranging from yeast to mice. The mutation of *Sch9*, which is homologous to *Akt*, extends the lifespan of yeast [95] and mutations that decrease the activity of insulin/IGF-1-like pathway increase the longevity of fruit flies [96] and mice [97,98]. These mutations that extend the lifespan are associated with increased resistance to oxidative stress, which is mediated in part by an increase in expression of antioxidant genes [99–101]. In mammalian cells, activation of Akt has been reported to induce cell proliferation and survival toward tumorigenesis [102–104]. The insulin pathway has also been shown to be essential for the maintenance of normal metabolic homeostasis [105]. Restriction of caloric intake extends the longevity of yeast, worms, fruit flies, mice and probably humans and postpones or prevents age-dependent deterioration and chronic diseases [91]. Since calorie restriction associates with the persistent decrease in the insulin signals, one might think that the insulin pathway could be involved in human aging and age-associated diseases, especially in the patients with diabetes.

Mice models that exhibit an early onset of phenotypes associated with aging have been reported. These include mouse mutants carrying targeted disruption of the genes involving DNA damage repair, such as *ku86* [106], *XPD* [107] and *BRCA1* [108]. Activation of p53 [109] as well as telomerase deficiency [58] also cause premature aging, which is characterized by reduced longevity, osteoporosis, organ atrophy and a diminished stress tolerance. All these molecules have been implicated in cellular senescence. More importantly, cellular senescence in vivo has been detected in premature aging mice [108]. Thus, these results provide in vivo evidence that links cellular senescence to organismal aging.

11. Conclusion

Accumulating evidence indicates a critical role of cellular senescence in organismal aging and age-related disease including atherosclerosis. Young adult bone marrow-derived EPCs have been shown to restore aging-impaired angiogenic function [110]. Chronic treatment with EPCs from young non-atherosclerotic ApoE-deficient mice prevents atherosclerosis progression in ApoE-deficient recipients despite persistent hypercholesterolemia [111]. Moreover, introduction of telomerase into EPCs has been reported to extend cell lifespan and to increase the efficacy of vasculogenesis in vivo [112]. These reports indicate that progressive progenitor cell deficits contribute to age-associated vascular dysfunction and suggest the potential utility of cell-based antisenescence therapy as a novel therapeutic strategy for vascular aging. Further understanding of mechanisms underlying cellular senescence will provide new insights into the pathogenesis of age-associated vascular disorders.

Acknowledgements

This work was supported by a Grant-in-Aid for Scientific Research, Developmental Scientific Research and Scientific Research on Priority Areas from the Ministry of Education, Science, Sports and Culture, the Program for Promotion of Fundamental Studies in Health Sciences of the Organization for Drug ADR Relief, R&D Promotion and Product Review of Japan (to I.K.) and grants from Takeda Medical Research Foundation, Takeda Science Foundation, Japan Heart Foundation, Mochida Memorial Foundation, Uehara Memorial

Foundation, Mitsubishi Pharma Research Foundation and the Ministry of Education, Science, Sports and Culture of Japan (to T.M.).

References

[1] Faragher RG, Kipling D. How might replicative senescence contribute to human ageing? Bioessays 1998;20:985–91.

[2] Hayflick L. Current theories of biological aging. Fed Proc 1975;34:9–13.

[3] Schneider EL, Mitsui Y. The relationship between in vitro cellular aging and in vivo human age. Proc Natl Acad Sci USA 1976;73:3584–8.

[4] Rohme D. Evidence for a relationship between longevity of mammalian species and life spans of normal fibroblasts in vitro and erythrocytes in vivo. Proc Natl Acad Sci USA 1981;78:5009–13.

[5] Thompson KV, Holliday R. Genetic effects on the longevity of cultured human fibroblasts. II. DNA repair deficient syndromes. Gerontology 1983;29:83–8.

[6] Campisi J, Kim SH, Lim CS, Rubio M. Cellular senescence, cancer and aging: the telomere connection. Exp Gerontol 2001;36:1619–37.

[7] Serrano M, Blasco MA. Putting the stress on senescence. Curr Opin Cell Biol 2001;13:748–53.

[8] Serrano M, Lin AW, McCurrach ME, Beach D, Lowe SW. Oncogenic ras provokes premature cell senescence associated with accumulation of p53 and p16INK4a. Cell 1997;88:593–602.

[9] Lin AW, Barradas M, Stone JC, van Aelst L, Serrano M, Lowe SW. Premature senescence involving p53 and p16 is activated in response to constitutive MEK/MAPK mitogenic signaling. Genes Dev 1998;12:3008–19.

[10] Zhu J, Woods D, McMahon M, Bishop JM. Senescence of human fibroblasts induced by oncogenic Raf. Genes Dev 1998;12:2997–3007.

[11] Campisi J. The biology of replicative senescence. Eur J Cancer 1997;33:703–9.

[12] Bringold F, Serrano M. Tumor suppressors and oncogenes in cellular senescence. Exp Gerontol 2000;35:317–29.

[13] Dimri GP, Lee X, Basile G, Acosta M, Scott G, Roskelley C, et al. A biomarker that identifies senescent human cells in culture and in aging skin in vivo. Proc Natl Acad Sci USA 1995;92:9363–7.

[14] Kumazaki T, Kobayashi M, Mitsui Y. Enhanced expression of fibronectin during in vivo cellular aging of human vascular endothelial cells and skin fibroblasts. Exp Cell Res 1993;205:396–402.

[15] Bennett MR, Macdonald K, Chan SW, Boyle JJ, Weissberg PL. Cooperative interactions between RB and p53 regulate cell proliferation, cell senescence, and apoptosis in human vascular smooth muscle cells from atherosclerotic plaques. Circ Res 1998;82:704–12.

[16] Burrig KF. The endothelium of advanced arteriosclerotic plaques in humans. Arterioscler Thromb 1991;11:1678–89.

[17] Ross R, Wight TN, Strandness E, Thiele B. Human atherosclerosis. I. Cell constitution and characteristics of advanced lesions of the superficial femoral artery. Am J Pathol 1984;114:79–93.

[18] Fenton M, Barker S, Kurz DJ, Erusalimsky JD. Cellular senescence after single and repeated balloon catheter denudations of rabbit carotid arteries. Arterioscler Thromb Vasc Biol 2001;21:220–6.

[19] Minamino T, Miyauchi H, Yoshida T, Ishida Y, Yoshida H, Komuro I. Endothelial cell senescence in human atherosclerosis: role of telomere in endothelial dysfunction. Circulation 2002;105:1541–4.

[20] Minamino T, Yoshida T, Tateno K, Miyauchi H, Zou Y, Toko H, et al. Ras induces vascular smooth muscle cell senescence and inflammation in human atherosclerosis. Circulation, 2003 [in press].

[21] Marin J. Age-related changes in vascular responses: a review. Mech Ageing Dev 1995;79:71–114.

[22] Rivard A, Fabre JE, Silver M, Chen D, Murohara T, Kearney M, et al. Age-dependent impairment of angiogenesis. Circulation 1999;99:111–20.

[23] Rivard A, Berthou-Soulie L, Principe N, Kearney M, Curry C, Branellec D, et al. Age-dependent defect in vascular endothelial growth factor expression is associated with reduced hypoxia-inducible factor 1 activity. J Biol Chem 2000;275:29643–7.

[24] Schneiderman J, Sawdey MS, Keeton MR, Bordin GM, Bernstein EF, Dilley RB, et al. Increased type 1 plasminogen activator inhibitor gene expression in atherosclerotic human arteries. Proc Natl Acad Sci USA 1992;89:6998–7002.

[25] Sato I, Morita I, Kaji K, Ikeda M, Nagao M, Murota S. Reduction of nitric oxide producing activity associated with in vitro aging in cultured human umbilical vein endothelial cell. Biochem Biophys Res Commun 1993;195:1070–6.

[26] Matsushita H, Chang E, Glassford AJ, Cooke JP, Chiu CP, Tsao PS. eNOS activity is reduced in senescent human endothelial cells: preservation by hTERT immortalization. Circ Res 2001;89:793–8.

[27] Hoffmann J, Haendeler J, Aicher A, Rossig L, Vasa M, Zeiher AM, et al. Aging enhances the sensitivity of endothelial cells toward apoptotic stimuli: important role of nitric oxide. Circ Res 2001;89:709–15.

[28] Nakajima M, Hashimoto M, Wang F, Yamanaga K, Nakamura N, Uchida T, et al. Aging decreases the production of PGI2 in rat aortic endothelial cells. Exp Gerontol 1997;32:685–93.

[29] Comi P, Chiaramonte R, Maier JA. Senescence-dependent regulation of type 1 plasminogen activator inhibitor in human vascular endothelial cells. Exp Cell Res 1995;219:304–8.

[30] Maier JA, Statuto M, Ragnotti G. Senescence stimulates U937-endothelial cell interactions. Exp Cell Res 1993;208:270–4.

[31] Yang J, Chang E, Cherry AM, Bangs CD, Oei Y, Bodnar A, et al. Human endothelial cell life extension by telomerase expression. J Biol Chem 1999;274:26141–8.

[32] Asahara T, Murohara T, Sullivan A, Silver M, van der Zee R, Li T, et al. Isolation of putative progenitor endothelial cells for angiogenesis. Science 1997;275:964–7.

[33] Takahashi T, Kalka C, Masuda H, Chen D, Silver M, Kearney M, et al. Ischemia- and cytokine-induced mobilization of bone marrow-derived endothelial progenitor cells for neovascularization. Nat Med 1999;5:434–8.

[34] Hill JM, Zalos G, Halcox JP, Schenke WH, Waclawiw MA, Quyyumi AA, et al. Circulating endothelial progenitor cells, vascular function, and cardiovascular risk. New Engl J Med 2003;348:593–600.

[35] Vasa M, Fichtlscherer S, Aicher A, Adler K, Urbich C, Martin H, et al. Number and migratory activity of circulating endothelial progenitor cells inversely correlate with risk factors for coronary artery disease. Circ Res 2001;89:E1–7.

[36] Stewart SA, Ben-Porath I, Carey VJ, O'Connor BF, Hahn WC, Weinberg RA. Erosion of the telomeric single-strand overhang at replicative senescence. Nat Genet 2003;33:492–6.

[37] Karlseder J, Smogorzewska A, de Lange T. Senescence induced by altered telomere state, not telomere loss. Science 2002;295:2446–9.

[38] Bodnar AG, Ouellette M, Frolkis M, Holt SE, Chiu CP, Morin GB, et al. Extension of life-span by introduction of telomerase into normal human cells. Science 1998;279:349–52.

[39] Bryan TM, Englezou A, Dalla-Pozza L, Dunham MA, Reddel RR. Evidence for an alternative mechanism for maintaining telomere length in human tumors and tumor-derived cell lines. Nat Med 1997;3:1271–4.

[40] Chang E, Harley CB. Telomere length and replicative aging in human vascular tissues. Proc Natl Acad Sci USA 1995;92:11190–4.

[41] Minamino T, Mitsialis SA, Kourembanas S. Hypoxia extends the life span of vascular smooth muscle cells through telomerase activation. Mol Cell Biol 2001;21:3336–42.

[42] Blackburn EH. Switching and signaling at the telomere. Cell 2001;106:661–73.

[43] Baumann P, Cech TR. Pot1, the putative telomere end-binding protein in fission yeast and humans. Science 2001;292:1171–5.
[44] Hsu HL, Gilley D, Blackburn EH, Chen DJ. Ku is associated with the telomere in mammals. Proc Natl Acad Sci USA 1999;96:12454–8.
[45] Broccoli D, Smogorzewska A, Chong L, de Lange T. Human telomeres contain two distinct Myb-related proteins, TRF1 and TRF2. Nat Genet 1997;17:231–5.
[46] Loayza D, De Lange T. POT1 as a terminal transducer of TRF1 telomere length control. Nature 2003;424:1013–8.
[47] Espejel S, Franco S, Rodriguez-Perales S, Bouffler SD, Cigudosa JC, Blasco MA. Mammalian Ku86 mediates chromosomal fusions and apoptosis caused by critically short telomeres. EMBO J 2002;21: 2207–19.
[48] Espejel S, Franco S, Sgura A, Gae D, Bailey SM, Taccioli GE, et al. Functional interaction between DNA-PKCs and telomerase in telomere length maintenance. EMBO J 2002;21:6275–87.
[49] Wong KK, Maser RS, Bachoo RM, Menon J, Carrasco DR, Gu Y, et al. Telomere dysfunction and Atm deficiency compromises organ homeostasis and accelerates ageing. Nature 2003;421:643–8.
[50] Griffith JD, Comeau L, Rosenfield S, Stansel RM, Bianchi A, Moss H, et al. Mammalian telomeres end in a large duplex loop. Cell 1999;97:503–14.
[51] van Steensel B, Smogorzewska A, de Lange T. TRF2 protects human telomeres from end-to-end fusions. Cell 1998;92:401–13.
[52] Smogorzewska A, de Lange T. Different telomere damage signaling pathways in human and mouse cells. EMBO J 2002;21:4338–48.
[53] Baur JA, Zou Y, Shay JW, Wright WE. Telomere position effect in human cells. Science 2001;292:2075–7.
[54] Minamino T, Komuro I. Role of telomere in endothelial dysfunction in atherosclerosis. Curr Opin Lipidol 2002;13:537–43.
[55] Karlseder J, Broccoli D, Dai Y, Hardy S, de Lange T. p53-and ATM-dependent apoptosis induced by telomeres lacking TRF2. Science 1999;283:1321–5.
[56] Blasco MA, Lee HW, Hande MP, Samper E, Lansdorp PM, DePinho RA, et al. Telomere shortening and tumor formation by mouse cells lacking telomerase RNA. Cell 1997;91:25–34.
[57] Lee HW, Blasco MA, Gottlieb GJ, Horner II JW, Greider CW, DePinho RA. Essential role of mouse telomerase in highly proliferative organs. Nature 1998;392:569–74.
[58] Rudolph KL, Chang S, Lee HW, Blasco M, Gottlieb GJ, Greider C, et al. Longevity, stress response, and cancer in aging telomerase-deficient mice. Cell 1999;96:701–12.
[59] Franco S, Segura I, Riese HH, Blasco MA, Decreased B. Decreased B16F10 melanoma growth and impaired vascularization in telomerase-deficient mice with critically short telomeres. Cancer Res 2002;62:552–9.
[60] Leri A, Franco S, Zacheo A, Barlucchi L, Chimenti S, Limana F, et al. Ablation of telomerase and telomere loss leads to cardiac dilatation and heart failure associated with p53 upregulation. EMBO J 2003;22: 131–9.
[61] Kim NW, Piatyszek MA, Prowse KR, Harley CB, West MD, Ho PL, et al. Specific association of human telomerase activity with immortal cells and cancer. Science 1994;266:2011–5.
[62] Lin SY, Elledge SJ. Multiple tumor suppressor pathways negatively regulate telomerase. Cell 2003;113:881–9.
[63] Smith LL, Coller HA, Roberts JM. Telomerase modulates expression of growth-controlling genes and enhances cell proliferation. Nat Cell Biol 2003;5:474–9.
[64] Minamino T, Kourembanas S. Mechanisms of telomerase induction during vascular smooth muscle cell proliferation. Circ Res 2001;89: 237–43.
[65] Hsiao R, Sharma HW, Ramakrishnan S, Keith E, Narayanan R. Telomerase activity in normal human endothelial cells. Anticancer Res 1997;17:827–32.
[66] Yang J, Nagavarapu U, Relloma K, Sjaastad MD, Moss WC, Passaniti A, et al. Telomerized human microvasculature is functional in vivo. Nat Biotechnol 2001;19:219–24.
[67] Dimri GP, Itahana K, Acosta M, Campisi J. Regulation of a senescence checkpoint response by the E2F1 transcription factor and p14(ARF) tumor suppressor. Mol Cell Biol 2000;20:273–85.
[68] Wang W, Chen JX, Liao R, Deng Q, Zhou JJ, Huang S, et al. Sequential activation of the MEK-extracellular signal-regulated kinase and MKK3/6-p38 mitogen-activated protein kinase pathways mediates oncogenic ras-induced premature senescence. Mol Cell Biol 2002;22:3389–403.
[69] Sherr CJ. Tumor surveillance via the ARF-p53 pathway. Gene Dev 1998;12:2984–91.
[70] Palmero I, Pantoja C, Serrano M. p19ARF links the tumour suppressor p53 to Ras. Nature 1998;395:125–6.
[71] Jacobs JJ, Keblusek P, Robanus-Maandag E, Kristel P, Lingbeek M, Nederlof PM, et al. Senescence bypass screen identifies TBX2, which represses Cdkn2a (p19(ARF)) and is amplified in a subset of human breast cancers. Nat Genet 2000;26:291–9.
[72] Ferbeyre G, de Stanchina E, Querido E, Baptiste N, Prives C, Lowe SW. PML is induced by oncogenic ras and promotes premature senescence. Gene Dev 2000;14:2015–27.
[73] Pearson M, Carbone R, Sebastiani C, Cioce M, Fagioli M, Saito S, et al. PML regulates p53 acetylation and premature senescence induced by oncogenic Ras. Nature 2000;406:207–10.
[74] Chin L, Artandi SE, Shen Q, Tam A, Lee SL, Gottlieb GJ, et al. p53 deficiency rescues the adverse effects of telomere loss and cooperates with telomere dysfunction to accelerate carcinogenesis. Cell 1999;97: 527–38.
[75] Burkhart BA, Alcorta DA, Chiao C, Isaacs JS, Barrett JC. Two post-transcriptional pathways that regulate p21(Cip1/Waf1/Sdi1) are identified by HPV16-E6 interaction and correlate with life span and cellular senescence. Exp Cell Res 1999;247:168–75.
[76] Ohtani N, Zebedee Z, Huot TJ, Stinson JA, Sugimoto M, Ohashi Y, et al. Opposing effects of Ets and Id proteins on p16INK4a expression during cellular senescence. Nature 2001;409:1067–70.
[77] McConnell BB, Starborg M, Brookes S, Peters G. Inhibitors of cyclin-dependent kinases induce features of replicative senescence in early passage human diploid fibroblasts. Curr Biol 1998;8:351–4.
[78] Ihling C, Menzel G, Wellens E, Monting JS, Schaefer HE, Zeiher AM. Topographical association between the cyclin-dependent kinases inhibitor p21, p53 accumulation, and cellular proliferation in human atherosclerotic tissue. Arterioscler Thromb Vasc Biol 1997;17:2218–24.
[79] Guevara NV, Kim HS, Antonova EI, Chan L. The absence of p53 accelerates atherosclerosis by increasing cell proliferation in vivo. Nat Med 1999;5:335–9.
[80] von der Thusen JH, van Vlijmen BJ, Hoeben RC, Kockx MM, Havekes LM, van Berkel TJ, et al. Induction of atherosclerotic plaque rupture in apolipoprotein E-/-mice after adenovirus-mediated transfer of p53. Circulation 2002;105:2064–70.
[81] Lusis AJ. Atherosclerosis. Nature 2000;407:233–41.
[82] Indolfi C, Avvedimento EV, Rapacciuolo A, Di Lorenzo E, Esposito G, Stabile E, et al. Inhibition of cellular ras prevents smooth muscle cell proliferation after vascular injury in vivo. Nat Med 1995; 1:541–5.
[83] George J, Afek A, Keren P, Herz I, Goldberg I, Haklai R, et al. Functional inhibition of Ras by *S*-trans, trans-farnesyl thiosalicylic acid attenuates atherosclerosis in apolipoprotein E knockout mice. Circulation 2002;105:2416–22.
[84] Brasier AR, Recinos III A, Eledrisi MS. Vascular inflammation and the renin–angiotensin system. Arterioscler Thromb Vasc Biol 2002; 22:1257–66.
[85] Libby P, Ridker PM, Maseri A. Inflammation and atherosclerosis. Circulation 2002;105:1135–43.
[86] Guarente L, Kenyon C. Genetic pathways that regulate ageing in model organisms. Nature 2000;408:255–62.
[87] Kenyon C. A conserved regulatory system for aging. Cell 2001;105: 165–8.

[Cell Cycle 3:4, 449-451; April 2004]; ©2004 Landes Bioscience

Perspecticve

Akt-Induced Cellular Senescence

Implication for Human Disease

Tohru Minamino
Hideyuki Miyauchi
Kaoru Tateno
Takeshige Kunieda
Issei Komuro*

Department of Cardiovascular Science and Medicine; Chiba University Graduate School of Medicine; Chiba, Japan

*Correspondence to: Issei Komuro; Department of Cardiovascular Science and Medicine; Chiba University Graduate School of Medicine; 1-8-1 Inohana, Chuo-ku, Chiba 260-8670, Japan; Tel.: +81.43.226.2097; Fax: +81.43.226.2557; Email: komuro-tky@umin.ac.jp

Received 02/25/04; Accepted 02/26/04

Previously published online as a *Cell Cycle* E-publication: http://www.landesbioscience.com/journals/cc/abstract.php?id=819

KEY WORDS

Akt, insulin, diabetes mellitus, atherosclerosis, senescence

ABSTRACT

Reduction-of-function mutations in components of the insulin/insulin-like growth factor-1/Akt pathway have been shown to extend the lifespan in organisms ranging from yeast to mice. It has also been reported that activation of Akt induces proliferation and survival of mammalian cells, thereby promoting tumorigenesis. We have recently shown that Akt activity increases with cellular senescence and that inhibition of Akt extends the lifespan of primary cultured human endothelial cells. Constitutive activation of Akt promotes senescence-like arrest of cell growth via a p53/p21-dependent pathway, leading to endothelial dysfunction. This novel role of Akt in regulating the cellular lifespan may contribute to various human diseases including atherosclerosis and diabetes mellitus.

Normal human somatic cells have a finite lifespan in vitro and eventually show irreversible growth arrest called cellular senescence. As cells age in vitro, significant phenotypic changes occur. The cells become flattened and enlarged, as well as expressing different genes such as the tumor suppressor gene p53 and cyclin-dependent kinase inhibitors including $p21^{Waf1/Cip1}$ and $p16^{Ink4a}$.[1] Signals other than extended proliferation have also been shown to produce a phenotype which is indistinguishable from that of senescent cells at the end of their replicative lifespan.[2] For example, constitutive activation of mitogenic stimuli, DNA damage, or oxidative stress can all prematurely induce cellular senescence.[3-5] In senescent vascular cells, expression of pro-inflammatory molecules is increased and production of vasodilators is decreased,[6-9] both of which are well-known changes in the vascular tissues of elderly persons that contribute to the pathogenesis of vascular aging.[10] There is also in vivo evidence cellular senescence.[11,12] Vascular cells with a similar phenotype to that of senescent vascular cells in vitro have been detected in human atheroma tissues, but not in normal arteries.[6,7] Such reports suggest that cellular senescence may play an important role in human aging and age-associated diseases. Alternatively, the mechanisms underlying cellular senescence may also regulate the lifespan of the entire organism and vice versa. This concept is supported by recent studies on mice that exhibit early onset of phenotypes associated with aging. These include mouse mutants with targeted disruption of the genes that are involved in the repair of DNA damage, such as *ku86*,[13] *XPD*[14] and *BRCA1*.[15] Activation of p53 as well as telomerase-deficiency also cause premature aging,[16,17] which is characterized by reduced longevity, osteoporosis, organ atrophy and a diminished stress tolerance. All of these molecules have been implicated in cellular senescence. More importantly, cellular senescence has been detected in the tissues of mice with premature aging.[15] These results provide further in vivo evidence that links cellular senescence to aging of the organism.

Restriction of calorie intake is known to extend longevity in organisms ranging from yeast to mice and to prevent age-dependent deterioration such as cancer, impaired immune function, and increased inflammation.[18,19] Calorie restriction decreases the plasma levels of glucose, insulin, and insulin-like growth factor-1 (IGF-1). Recent genetic analyses have demonstrated that reduction-of-function mutations in the glucose or IGF-1-like signaling pathways also extend the lifespan of many organisms, suggesting that these pathways may underlie the mechanism of longevity related to calorie restriction.[18,20] Among the molecules that exist in these pathways, the Ser/Thr kinase Akt is remarkably well conserved across a broad range of species and is involved in a diverse array of cellular processes.[21] Although mutations that reduce Akt activity prolong the longevity of yeast and nematodes,[22,23] activation of Akt has been reported to induce proliferation and survival of mammalian cells, thereby promoting tumorigenesis.[21,24,25] In a study that was recently published in *EMBO J*,[26] we showed that Akt activity increases with cellular senescence and that inhibition of Akt extends the lifespan of primary cultured human endothelial cells.

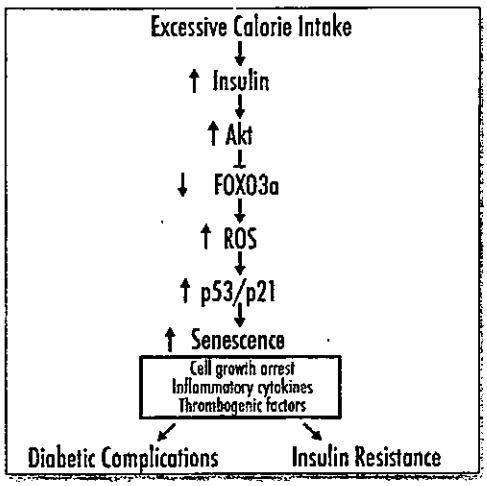

Figure 1. Signaling pathway of insulin/Akt-induced senescence. Excessive calorie intake increases the levels of insulin and results in activation of Akt in the target tissues. Constitutive activation of Akt induces cellular senescence via a p53/p21-dependent pathway, which is mediated by the forkhead transcription factor (FOXO3a), which regulates cellular levels of reactive oxygen species. Accumulation of senescent cells in the target organs causes diabetic complications and promotes insulin resistance because of their senescent phenotypes such as increased production of inflammatory cytokines and thrombogenic factors.

Constitutive activation of Akt promotes senescence-like arrest of cell growth via a p53/p21-dependent pathway. This action is at least partly mediated by the forkhead transcription factor, which regulates cellular levels of reactive oxygen species. Our findings reveal a novel role of Akt in regulating the cellular lifespan and suggest that the mechanism of longevity is conserved in primary cultured human cells.

What is the implication of these findings for human disease? Since various growth factors that contribute to atherosclerosis have been shown to increase Akt activity,[27] atherogenic stimuli may activate Akt in the vasculature and thus promote atherogenesis. Consistent with this notion, activation of Akt is observed in human atheroma tissues, but not in normal arteries.[26] Constitutive activation of Akt in human endothelial cells not only leads to cellular senescence but also to vascular dysfunction such as impaired angiogenesis and increased inflammation.[26] In a similar way, Akt-induced senescence may contribute to other age-associated diseases. Cell division is essential for the survival of multicellular organisms that contain various renewable tissues, but it also puts the organism at risk of developing cancer. Thus, complex organisms have evolved at least two cellular mechanisms to prevent oncogenesis, which are apoptosis and cellular senescence.[2] In this respect, Akt-induced senescence can be seen as an anti-tumorigenesis mechanism since gain-of-function mutations in the Akt signaling pathway are common in human cancers. Finally, Akt is known to be involved in signaling pathways that mediate the metabolic effects of insulin in several physiologically important target tissues.[28] Insulin regulates energy metabolism after food intake by promoting the uptake and storage of glucose, amino acid and fat, while simultaneously antagonizing the catabolism of fuel reserve. The basic role of insulin as a signal that informs the organism of nutritional abundance appears to be well conserved among species.[28] We have shown that insulin also increases p53 activity and expression of p21 and that it promotes cellular senescence in an Akt-dependent manner.[26] Since hyperinsulinemia is a basic feature of type 2 diabetes mellitus, insulin-induced senescence may have the direct impact on diabetic complications such as vasculopathy and nephropathy. An inevitable feature of type 2 diabetes mellitus is insulin resistance.[28] Some previous studies have suggested that a decline of Akt activity in response to insulin might lead to insulin resistance.[29] In contrast, some recent studies have shown that basal Akt activity in the tissues of diabetic patients tends to be higher than in normal subjects and that there is no significant difference in the response of Akt to insulin stimulation.[30] Increased plasma and tissue levels of pro-inflammatory cytokines and pro-thrombogenic factors have been demonstrated to exaggerate insulin resistance and to contribute to diabetic complications,[31,32] and both of these changes are well-known features of senescent cells in vitro.[12] Accordingly, we propose that type 2 diabetes mellitus can be regarded as a premature aging syndrome in which the dysregulation of insulin/Akt signaling promotes cellular senescence, leading to various complications. This suggests that anti-senescence therapy might be effective for the treatment of diabetic complications and insulin resistance.

References

1. Faragher RG, Kipling D. How might replicative senescence contribute to human ageing? Bioessays 1998; 20:985-91.
2. Serrano M, Blasco MA. Putting the stress on senescence. Curr Opin Cell Biol 2001; 13:748-53.
3. Chen Q, Ames BN. Senescence-like growth arrest induced by hydrogen peroxide in human diploid fibroblast F65 cells. Proc Natl Acad Sci USA 1994; 91:4130-4.
4. Chen Q, Fischer A, Reagan JD, Yan LJ, Ames BN. Oxidative DNA damage and senescence of human diploid fibroblast cells. Proc Natl Acad Sci USA 1995; 92:4337-41.
5. Serrano M, Lin AW, McCurrach ME, Beach D, Lowe SW. Oncogenic ras provokes premature cell senescence associated with accumulation of p53 and $p16^{INK4a}$. Cell 1997; 88:593-602.
6. Minamino T, Miyauchi H, Yoshida T, Ishida Y, Yoshida H, Komuro I. Endothelial cell senescence in human atherosclerosis: role of telomere in endothelial dysfunction. Circulation 2002; 105:1541-4.
7. Minamino T, Yoshida T, Tateno K, Miyauchi H, Zou Y, Toko H, et al. Ras induces vascular smooth muscle cell senescence and inflammation in human atherosclerosis. Circulation 2003; 108:2264-9.
8. Matsushita H, Chang E, Glassford AJ, Cooke JP, Chiu CP, Tsao PS. eNOS activity is reduced in senescent human endothelial cells: Preservation by hTERT immortalization. Circ Res 2001; 89:793-8.
9. Nakajima M, Hashimoto M, Wang F, Yamanaga K, Nakamura N, Uchida T, et al. Aging decreases the production of PGI2 in rat aortic endothelial cells. Exp Gerontol 1997; 32:685-93.
10. Lusis AJ. Atherosclerosis. Nature 2000; 407:233-41.
11. Minamino T, Komuro I. Role of telomere in endothelial dysfunction in atherosclerosis. Curr Opin Lipidol 2002; 13:537-43.
12. Minamino T, Miyauchi H, Yoshida T, Tateno K, Kunieda T, Komuro I. Vascular cell senescence and vascular aging. J Mol Cell Cardiol 2004; 36:175-83.
13. Vogel H, Lim DS, Karsenty G, Finegold M, Hasty P. Deletion of Ku86 causes early onset of senescence in mice. Proc Natl Acad Sci USA 1999; 96:10770-5.
14. de Boer J, Andressoo JO, de Wit J, Huijmans J, Beems RB, van Steeg H, et al. Premature aging in mice deficient in DNA repair and transcription. Science 2002; 296:1276-9.
15. Cao L, Li W, Kim S, Brodie SG, Deng CX. Senescence, aging, and malignant transformation mediated by p53 in mice lacking the Brca1 full-length isoform. Genes Dev 2003; 17:201-13.
16. Tyner SD, Venkatachalam S, Choi J, Jones S, Ghebranious N, Igelmann H, et al. p53 mutant mice that display early ageing-associated phenotypes. Nature 2002; 415:45-53.
17. Rudolph KL, Chang S, Lee HW, Blasco M, Gottlieb GJ, Greider C, et al. Longevity, stress response, and cancer in aging telomerase-deficient mice. Cell 1999; 96:701-12.
18. Longo VD, Finch CE. Evolutionary medicine: from dwarf model systems to healthy centenarians? Science 2003; 299:1342-6.
19. Koubova J, Guarente L. How does calorie restriction work? Genes Dev 2003; 17:313-21.
20. Kenyon C. A conserved regulatory system for aging. Cell 2001; 105:165-8.
21. Datta SR, Brunet A, Greenberg ME. Cellular survival: a play in three Akts. Genes Dev 1999; 13:2905-27.
22. Fabrizio P, Pozza F, Pletcher SD, Gendron CM, Longo VD. Regulation of longevity and stress resistance by Sch9 in yeast. Science 2001; 292:288-90.
23. Kenyon C, Chang J, Gensch E, Rudner A, Tabtiang RA. C. elegans mutant that lives twice as long as wild type. Nature 1993; 366:461-4.
24. Blume-Jensen P, Hunter T. Oncogenic kinase signalling. Nature 2001; 411:355-65.
25. Testa JR, Bellacosa A. AKT plays a central role in tumorigenesis. Proc Natl Acad Sci USA 2001; 98:10983-5.

26. Miyauchi H, Minamino T, Tateno K, Kunieda T, Toko H, Komuro I. Akt negatively regulates the in vitro lifespan of human endothelial cells via a p53/p21-dependent pathway. EMBO J 2004; 23:212-20.
27. Cantley LC. The phosphoinositide 3-kinase pathway. Science. 2002;296:1655-7.
28. Whiteman EL, Cho H, Birnbaum MJ. Role of Akt/protein kinase B in metabolism. Trends Endocrinol Metab 2002; 13:444-51.
29. Krook A, Roth RA, Jiang XJ, Zierath JR, Wallberg-Henriksson H. Insulin-stimulated Akt kinase activity is reduced in skeletal muscle from NIDDM subjects. Diabetes 1998; 47:1281-6.
30. Hojlund K, Staehr P, Hansen BF, Green KA, Hardie DG, Richter EA, et al. Increased phosphorylation of skeletal muscle glycogen synthase at NH2-terminal sites during physiological hyperinsulinemia in type 2 diabetes. Diabetes 2003; 52:1393-402.
31. Rui L, Aguirre V, Kim JK, Shulman GI, Lee A, Corbould A, et al. Insulin/IGF-1 and TNF-α stimulate phosphorylation of IRS-1 at inhibitory Ser307 via distinct pathways. J Clin Invest 2001; 107:181-9.
32. Shimomura I, Funahashi T, Takahashi M, Maeda K, Kotani K, Nakamura T, et al. Enhanced expression of PAI-1 in visceral fat: possible contributor to vascular disease in obesity. Nat Med 1996; 2:800-3.

nature medicine

G-CSF prevents cardiac remodeling after myocardial infarction by activating the Jak-Stat pathway in cardiomyocytes

Mutsuo Harada[1,4], Yingjie Qin[1,4], Hiroyuki Takano[1,4], Tohru Minamino[1,4], Yunzeng Zou[1], Haruhiro Toko[1], Masashi Ohtsuka[1], Katsuhisa Matsuura[1], Masanori Sano[1], Jun-ichiro Nishi[1], Koji Iwanaga[1], Hiroshi Akazawa[1], Takeshige Kunieda[1], Weidong Zhu[1], Hiroshi Hasegawa[1], Keita Kunisada[2], Toshio Nagai[1], Haruaki Nakaya[3], Keiko Yamauchi-Takihara[2] & Issei Komuro[1]

Granulocyte colony-stimulating factor (G-CSF) was reported to induce myocardial regeneration by promoting mobilization of bone marrow stem cells to the injured heart after myocardial infarction, but the precise mechanisms of the beneficial effects of G-CSF are not fully understood. Here we show that G-CSF acts directly on cardiomyocytes and promotes their survival after myocardial infarction. G-CSF receptor was expressed on cardiomyocytes and G-CSF activated the Jak/Stat pathway in cardiomyocytes. The G-CSF treatment did not affect initial infarct size at 3 d but improved cardiac function as early as 1 week after myocardial infarction. Moreover, the beneficial effects of G-CSF on cardiac function were reduced by delayed start of the treatment. G-CSF induced antiapoptotic proteins and inhibited apoptotic death of cardiomyocytes in the infarcted hearts. G-CSF also reduced apoptosis of endothelial cells and increased vascularization in the infarcted hearts, further protecting against ischemic injury. All these effects of G-CSF on infarcted hearts were abolished by overexpression of a dominant-negative mutant Stat3 protein in cardiomyocytes. These results suggest that G-CSF promotes survival of cardiac myocytes and prevents left ventricular remodeling after myocardial infarction through the functional communication between cardiomyocytes and noncardiomyocytes.

Myocardial infarction is the most common cause of cardiac morbidity and mortality in many countries, and left ventricular remodeling after myocardial infarction is important because it causes progression to heart failure. Several cytokines including G-CSF, erythropoietin and leukemia inhibitory factor have beneficial effects on cardiac remodeling after myocardial infarction[1–5]. In particular, G-CSF markedly improves cardiac function and reduce mortality after myocardial infarction in mice, possibly by regeneration of myocardium and angiogenesis[1,2,6–8]. G-CSF is known to have various functions such as induction of proliferation, survival and differentiation of hematopoietic cells, as well as mobilization of bone marrow cells[9–11]. Although it was reported that bone marrow cells could differentiate into cardiomyocytes and vascular cells, thereby contributing to regeneration of myocardium and angiogenesis in ischemic hearts[12–15], accumulating evidence has questioned these previous reports[16–18]. In this study, we examined the molecular mechanisms of how G-CSF prevents left ventricular remodeling after myocardial infarction.

RESULTS

G-CSF directly acts on cultured cardiomyocytes

G-CSF receptor (G-CSFR, encoded by *CSF3R*) has been reported to be expressed only on blood cells such as myeloid leukemic cells, leukemic cell lines, mature neutrophils, platelets, monocytes and some lymphoid cell lines[9]. To test whether G-CSFR is expressed on mouse cardiomyocytes, we performed a reverse transcription–polymerase chain reaction (RT-PCR) experiment by using specific primers for mouse *Csf3r*. We detected expression of the *Csf3r* gene in the adult mouse heart and cultured neonatal cardiomyocytes (**Fig. 1a**). We next examined expression of G-CSFR protein in cultured cardiomyocytes of neonatal rats by immunocytochemistry. Similar to the previously reported expression pattern of G-CSFR in living cells[19], the immunoreactivity for G-CSFR was localized to the cytoplasm and cell membrane under steady-state conditions in cardiomyocytes (**Fig. 1b**). This immunoreactivity disappeared when the antibody specific for G-CSFR was omitted, validating its specificity (**Fig. 1b**). In addition to cardiomyocytes, we also detected expression of G-CSFR on cardiac fibroblasts by immunocytochemistry (see **Supplementary Fig. 1** online) and RT-PCR (**Supplementary Fig. 2** online).

The binding of G-CSF to its receptor has been reported to evoke signal transduction by activating the receptor-associated Janus family tyrosine kinases (JAK) and signal transducer and activator of transcription (STAT) proteins in hematopoietic cells[9,10]. In particular, STAT3

[1]Department of Cardiovascular Science and Medicine, Chiba University Graduate School of Medicine, 1-8-1 Inohana, Chuo-ku, Chiba 260-8670, Japan. [2]Department of Molecular Medicine, Osaka University Medical School, Osaka University, 2-2 Yamadaoka, Suita, Osaka 565-0871, Japan. [3]Department of Pharmacology, Chiba University Graduate School of Medicine, 1-8-1 Inohana, Chuo-ku, Chiba 260-8670, Japan. [4]These authors contributed equally to this work. Correspondence should be addressed to I.K. (komuro-tky@umin.ac.jp).

Published online 20 February 2005; doi:10.1038/nm1199

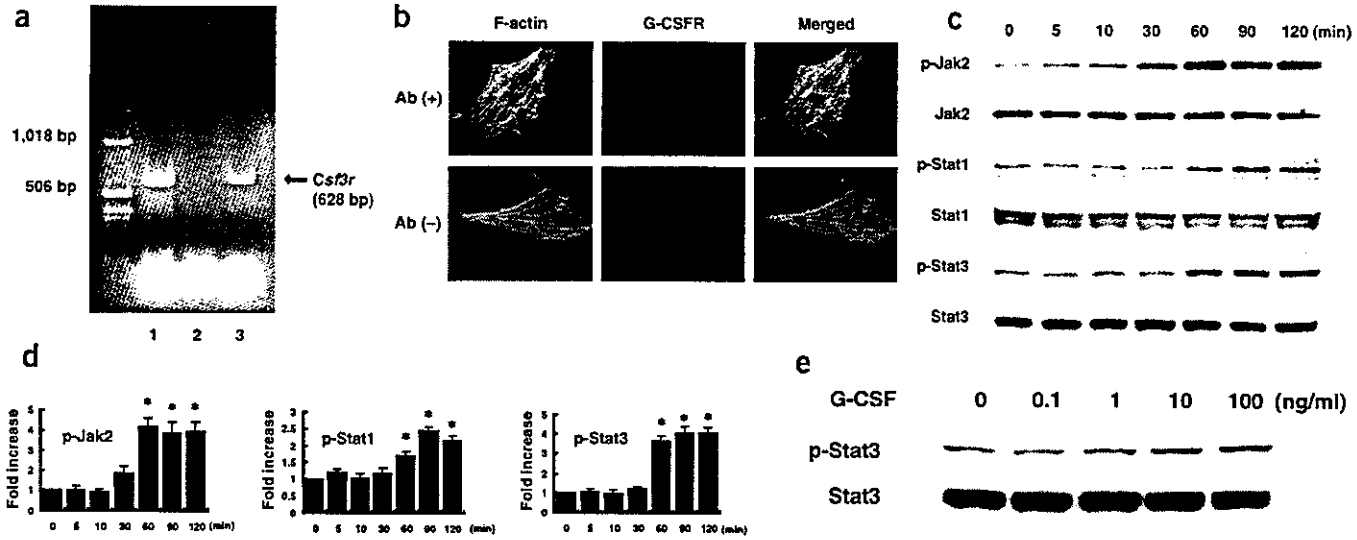

Figure 1 Expression of G-CSFR and the G-CSF-evoked signal transduction in cultured cardiomyocytes. (a) RT-PCR for mouse *Csf3r*. Expression of *Csf3r* was detected in the adult mouse heart (lane 1) and cultured cardiomyocytes of neonatal mice (lane 3). In lane 2, reverse transcription products were omitted to exclude the possibility of false-positive results from contamination. (b) Immunocytochemical staining for G-CSFR. Cardiomyocytes from neonatal rats were incubated with antibody to G-CSFR (red) and phalloidin (green) (upper panel). In the absence of antibody to G-CSFR, no signal was detected (lower panel). Original magnification, ×1,000. (c) G-CSF induces phosphorylation of Jak2, Stat1 and Stat3 in a time-dependent manner in cultured cardiomyocytes. (d) Quantification of Jak2, Stat1 and Stat3 activation by G-CSF stimulation as compared with control (time = 0). $^*P < 0.05$ versus control ($n = 3$). (e) G-CSF induces phosphorylation and activation of Stat3 in a dose-dependent manner in cultured cardiomyocytes.

has been reported to contribute to G-CSF-induced myeloid differentiation and survival[20,21]. We therefore examined whether G-CSF activates the Jak-Stat signaling pathway in cultured cardiomyocytes. G-CSF (100 ng/ml) significantly induced phosphorylation and activation of Jak2 and Stat3, and to a lesser extent, Stat1 but not Jak1, Tyk2 or Stat5 in a dose-dependent manner (Fig. 1c–e and data not shown), suggesting that G-CSFR on cardiomyocytes is functional.

We next examined whether G-CSF confers direct protective effects on cardiomyocytes as it prevents hematopoietic cells from apoptotic death[21]. We exposed cardiomyocytes to 0.1 mM H_2O_2 in the absence or presence of G-CSF and examined cardiomyocyte apoptosis by staining with annexin V[22,23]. Pretreatment with G-CSF significantly reduced the number of H_2O_2-induced annexin V–positive cells compared with cells that were not given the G-CSF pretreatment

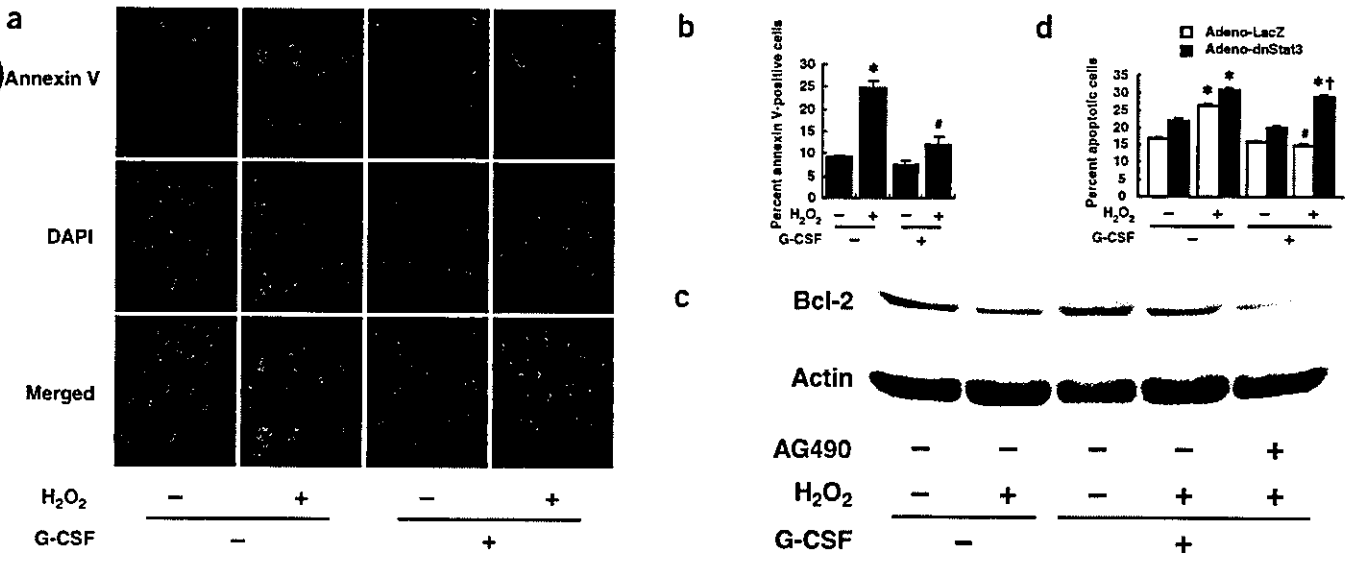

Figure 2 Suppression of H_2O_2-induced cardiomyocyte apoptosis by G-CSF. (a) Detection of apoptosis by Cy3-labeled annexin V. Red fluorescence shows apoptotic cardiomyocytes stained with Cy3-labeled annexin V. Nuclei were counterstained with DAPI staining (blue). Original magnification, ×400. (b) Quantitative analysis of apoptotic cells. The vertical axis indicates the ratio of the annexin V–positive cell number relative to that of DAPI-positive nuclei. $^*P < 0.01$ versus nontreated cells, $^\#P < 0.05$ versus H_2O_2-treated cells without G-CSF ($n = 3$). (c) G-CSF prevents H_2O_2-induced downregulation of Bcl-2 expression ($n = 3$). (d) Inhibition of antiapoptotic effects of G-CSF by Adeno-dnStat3. Bar graphs represent quantitative analysis of the apoptotic cell number relative to the total cell number. $^*P < 0.001$ versus H_2O_2 (–)/G-CSF (–), $^\#P < 0.001$ versus H_2O_2 (+)/G-CSF (–), $^\dagger P < 0.001$ versus H_2O_2 (+)/G-CSF (+)/Adeno-LacZ ($n = 3$).

(Fig. 2a,b). To investigate the molecular mechanism of how G-CSF exerts an antiapoptotic effect on cultured cardiomyocytes, we examined expression of the Bcl-2 protein family, known target molecules of the Jak-Stat pathway[24], by western blot analysis. Expression levels of antiapoptotic proteins such as Bcl-2 and Bcl-xL were lower when cardiomyocytes were subjected to H_2O_2 (Fig. 2c and data not shown), and this reduction was considerably inhibited by G-CSF pretreatment (Fig. 2c). AG490, an inhibitor of Jak2, abolished G-CSF-induced Bcl-2 expression (Fig. 2c) but did not affect its basal levels (**Supplementary Fig. 3** online), suggesting a crucial role of the Jak-Stat pathway in inducing survival of cardiomyocytes by G-CSF. To further elucidate the involvement of the Jak-Stat pathway in the protective effects of G-CSF on cardiomyocytes, we transduced cultured cardiomyocytes with adenovirus encoding dominant-negative Stat3 (Adeno-dnStat3). G-CSF treatment significantly reduced apoptosis induced by H_2O_2 in Adeno-LacZ-infected cardiomyocytes (Fig. 2d). This effect was abolished by introduction of Adeno-dnStat3 (Fig. 2d), suggesting that Stat3 mediates the protective effects of G-CSF on H_2O_2-induced cardiomyocyte apoptosis.

Effects of G-CSF on cardiac function after myocardial infarction

Consistent with the *in vitro* data, G-CSF enhanced activation of Stat3 in the infarcted heart (Fig. 3a). Notably, the levels of G-CSFR were markedly increased after myocardial infarction in cardiomyocytes (**Supplementary Fig. 4** online), which may enhance the effects of G-CSF on the infarcted heart. To elucidate the role of G-CSF-induced Stat3 activation in cardiac remodeling, we produced myocardial infarction in transgenic mice which express dominant-negative Stat3 in cardiomyocytes under the control of the α-myosin heavy chain promoter (dnStat3-Tg). Administration of G-CSF was started at the time of coronary artery ligation (day 0) until day 4 in transgenic mice; we termed this group Tg-G mice. A control group of dnStat3-Tg mice given myocardial infarction received saline (Tg-cont) instead of G-CSF. We also included two groups of wild-type mice given myocardial infarction treated with G-CSF (Wt-G) or saline (Wt-cont). At 2 weeks after myocardial infarction, we assessed the morphology by histological analysis and measured cardiac function by echocardiography and catheterization analysis. The infarct area was significantly smaller in the Wt-G group than the Wt-cont group (Fig. 3b). The Wt-G group also showed less left ventricular end-diastolic dimension (LVEDD) and better fractional shortening as assessed by echocardiography, and lower end-diastolic pressure (LVEDP) and better $+dp/dt$ and $-dp/dt$ as assessed by cardiac catheterization compared with Wt-cont (Fig. 3c). The beneficial effects of G-CSF on cardiac function were dose dependent and were significantly reduced by delayed start of the treatment (Fig. 3d,e and **Supplementary Fig. 5** online). Moreover, its favorable effects on cardiac function became evident within 1 week after the treatment (Fig. 3f). Disruption of the Stat3 signaling pathway in cardiomyocytes abolished the protective effects of G-CSF. There was no significant difference in LVEDD, fractional shortening, LVEDP, $+dp/dt$ and $-dp/dt$ between Tg-G and Tg-cont (Fig. 3c). We obtained similar results from infarcted female hearts (Fig. 3g). These results suggest that G-CSF protects the heart after myocardial infarction at least in part by directly activating Stat3 in cardiomyocytes, which is a gender-independent effect. We have previously shown that treatment with G-CSF significantly ($P < 0.05$) decreased myocardial infarction–related mortality of wild-type mice[2]. In contrast, there were no significant differences in mortality between G-CSF-treated and saline-treated dnStat3-Tg mice (data not shown).

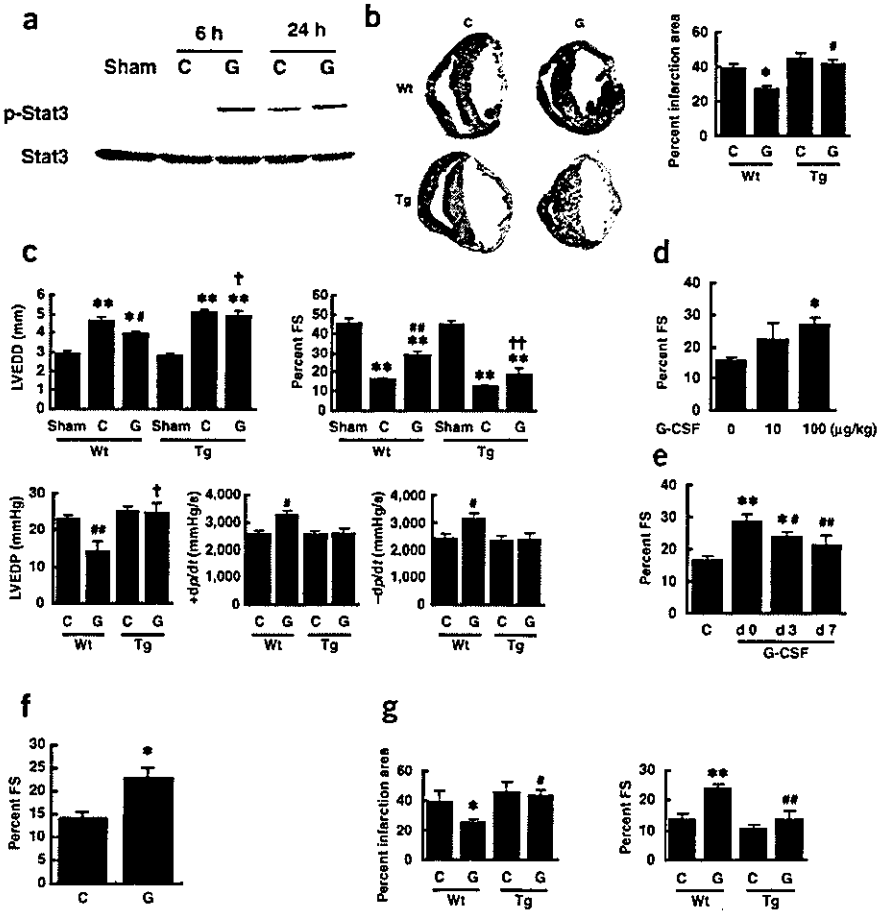

Figure 3 Effects of G-CSF on cardiac function after myocardial infarction. (a) Stat3 activation in the infarcted hearts. We operated on wild-type mice to induce myocardial infarction and treated them with G-CSF (G) or saline (C). (b) Masson trichrome staining of wild-type (Wt) and dnStat3-Tg (Tg) hearts. $^{*}P < 0.001$ versus Wt-cont, $^{\#}P < 0.001$ versus Wt-G ($n = 11$–15). (c) G-CSF treatment preserves cardiac function after myocardial infarction. $^{*}P < 0.01$, $^{**}P < 0.001$ versus sham; $^{\#}P < 0.05$, $^{\#\#}P < 0.001$ versus Wt-cont; $^{\dagger}P < 0.01$, $^{\dagger\dagger}P < 0.001$ versus Wt-G ($n = 10$–15 for echocardiography and $n = 5$ for catheterization analysis). (d) Dose-dependent effects of G-CSF. FS, fractional shortening. $^{*}P < 0.01$ versus saline-treated mice (G-CSF = 0)($n = 12$–14). (e) Wild-type mice were operated to induce myocardial infarction and G-CSF treatment (100 μg/kg/d) was started from the indicated day for 5 d. $^{*}P < 0.05$, $^{**}P < 0.001$ versus saline-treated mice (C); $^{\#}P < 0.05$, $^{\#\#}P < 0.01$ versus mice treated at day 0 (d 0) ($n = 11$–12). (f) Effects of G-CSF on cardiac function at 1 week. $^{*}P < 0.05$ versus control ($n = 3$). (g) Effects of G-CSF on cardiac function of female mice. $^{*}P < 0.05$, $^{**}P < 0.001$ versus Wt-cont; $^{\#}P < 0.05$, $^{\#\#}P < 0.005$ versus Wt-G ($n = 4$–5).

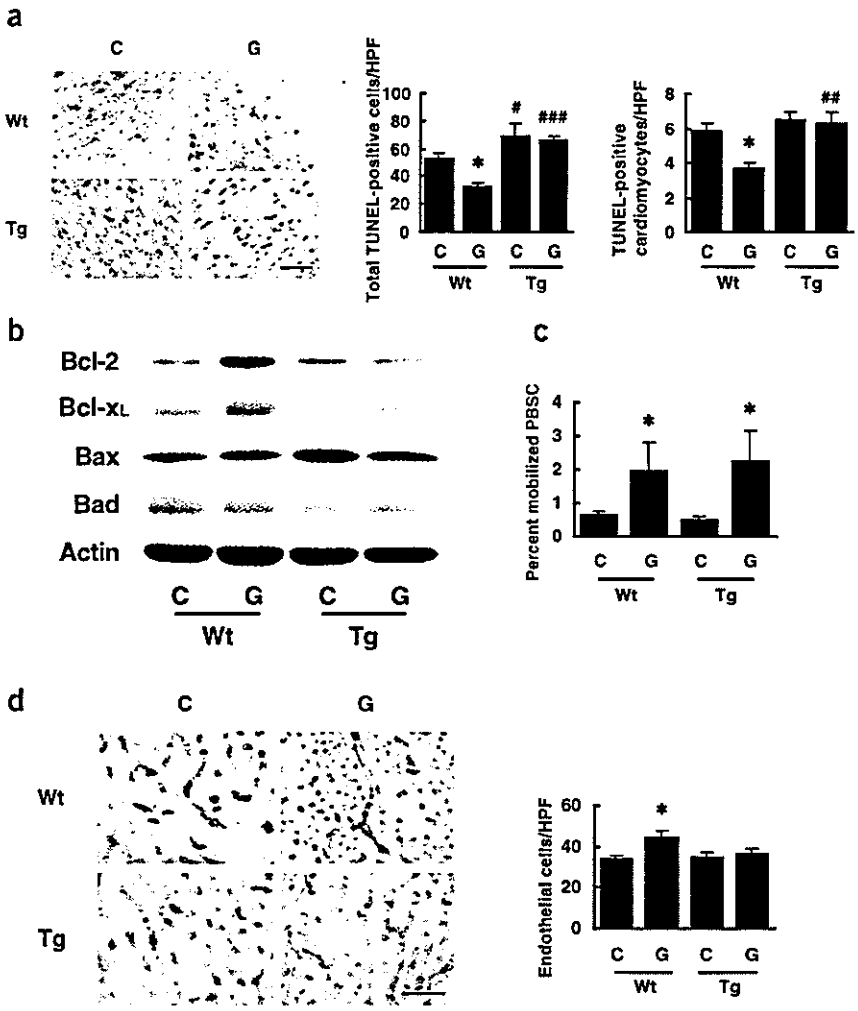

Figure 4 Mechanisms of the protective effects of G-CSF. (a) TUNEL staining (brown nuclei) in the infarcted hearts. The graphs show quantitative analyses for total TUNEL-positive cells (left graph) and TUNEL-positive cardiomyocytes (right graph) in infarcted hearts. $^{*}P < 0.01$ versus Wt-cont; $^{\#}P < 0.05$, $^{\#\#}P < 0.005$, $^{\#\#\#}P < 0.001$ versus wild-type mice with the same treatment ($n = 5$–7). Scale bar, 100 μm. (b) Infarcted hearts treated with G-CSF (G) or saline (C) were analyzed for expression of Bcl-2, Bcl-xL, Bax and Bad by western blotting ($n = 3$). (c) Mobilization of hematopoietic stem cells into peripheral blood (PBSC). $^{*}P < 0.05$ versus saline-treated mice ($n = 4$). (d) Capillary endothelial cells were identified by immunohistochemical staining with anti-PECAM antibody in the border zone of the infarcted hearts. Scale bar, 100 μm. The number of endothelial cells was counted and shown in the graph ($n = 6$–8). $^{*}P < 0.05$.

Mechanisms of the protective effects of G-CSF

Our *in vitro* results suggest that the protective effects of G-CSF on cardiac remodeling after myocardial infarction can be attributed in part to reduction of cardiomyocyte apoptosis. To determine whether the Stat3 pathway in cardiomyocytes mediates the antiapoptotic effects of G-CSF on the ischemic myocardium, we carried out TUNEL labeling of left ventricular sections 24 h after myocardial infarction in wild-type mice and dnStat3-Tg mice. Although the number of TUNEL-positive cells was significantly less in the Wt-G group than the Wt-cont group, G-CSF treatment had no effect on cardiomyocyte apoptosis in dnStat3-Tg mice (**Fig. 4a**). The effects of G-CSF on apoptosis after myocardial infarction were also attenuated when mice were treated with AG490 (**Supplementary Fig. 6** online). Myocardial infarction–related apoptosis was significantly increased in the Tg-cont group and AG490-treated wild-type mice compared with Wt-cont mice (**Fig. 4a** and **Supplementary Fig. 6** online), suggesting that endogenous activation of Stat3 has a protective role in the infarcted heart, as reported previously[25]. It is noteworthy that G-CSF treatment inhibited apoptosis of noncardiomyocytes including endothelial cells and that this inhibition was abolished in dnStat3-Tg mice (**Fig. 4a** and data not shown). To investigate the underlying molecular mechanism of the antiapoptotic effects of G-CSF *in vivo*, we examined expression of the Bcl-2 protein family by western blot analysis. Consistent with our *in vitro* results, expression of antiapoptotic proteins such as Bcl-2 and Bcl-xL was significantly increased in the Wt-G group at 24 h after myocardial infarction compared with the Wt-cont group, whereas expression of the proapoptotic proteins Bax and Bad was not affected by the treatment (**Fig. 4b**). In contrast, expression levels of antiapoptotic proteins were not increased by G-CSF in the Tg-G group (**Fig. 4b**). Immunohistochemical analysis also showed increased expression of Bcl-2 in the infarcted heart of the Wt-G group but not of the Tg-G group (**Supplementary Fig. 7** online).

To determine the effects of G-CSF on mobilization of stem cells, we counted the number of cells positive for both Sca-1 and c-kit in peripheral blood samples from mice treated with G-CSF or saline. The G-CSF treatment similarly increased the number of double-positive cells in wild-type mice and dnStat3-Tg mice (**Fig. 4c**). To examine the impact of G-CSF on cardiac homing of bone marrow cells, we transplanted bone marrow cells derived from GFP transgenic mice into wild-type and dnStat3-Tg mice, produced myocardial infarction and treated with G-CSF or saline. FACS analysis showed that G-CSF did not increase cardiac homing of bone marrow cells in wild-type and dnStat3-Tg mice (**Supplementary Fig. 8** online). We have shown that cardiac stem cells, which are able to differentiate into cardiomyocytes, exist in Sca-1-positive populations in the adult myocardium[26]. But G-CSF treatment did not affect the number of Sca-1-positive cells in the infarcted hearts of wild-type or dnStat3-Tg mice (**Supplementary Fig. 9** online). Thus, it is unlikely that G-CSF exerts its beneficial effects through expansion of cardiac stem cells. To determine the effects of G-CSF on proliferation of cardiomyocytes, we carried out immunostaining for Ki67, a marker for cell cycling, in conjunction with a labeling for troponin T. The number of Ki67-positive cardiomyocytes was increased in the infarcted hearts of wild-type mice and dnStat3-Tg mice compared with sham-operated mice (**Supplementary Fig. 10** online). But G-CSF did not alter the number of Ki67-positive cardiomyocytes in wild-type or dnStat3-Tg mice, suggesting that G-CSF does not induce proliferation of cardiomyocytes (**Supplementary Fig. 10** online). The number of Ki67-positive cardiomyocytes was less in infarcted hearts of dnStat3-Tg mice than in those of wild-type mice, suggesting that endogenous Stat3 activity is required

for myocardial regeneration after myocardial infarction and that activation of Stat3 by G-CSF is not sufficient for cardiomyocytes to enter the cell cycle in infarcted hearts of wild-type mice (**Supplementary Fig. 10** online). In contrast, G-CSF treatment significantly increased the number of endothelial cells in the border zone of the infarcted hearts (**Fig. 4d**). This increase was attenuated in dnStat3-Tg mice, indicating that the increased vascularity is mediated by Stat3 activity in cardiomyocytes and may partially account for the beneficial effects of G-CSF on the infarcted hearts. Taken together with the result that G-CSF-induced inhibition of noncardiomyocyte apoptosis was also mediated by the Stat3 signaling pathway in cardiomyocytes (**Fig. 4a**), these findings imply that communication between cardiomyocytes and noncardiomyocytes regulates each others' survival.

To further test whether G-CSF acts directly on the heart, we examined the effects of G-CSF treatment on cardiac function after ischemia-reperfusion injury in a Langendorff perfusion model. The isolated hearts underwent 30 min total ischemia followed by 120 min reperfusion with the perfusate containing G-CSF (300 ng/ml) or vehicle, and left ventricular developed pressure (LVDP, measured as the difference between systolic and diastolic pressures of the left ventricle) and LVEDP were measured. There were no significant differences in basal hemodynamic parameters including heart rate, left ventricular pressure, LVEDP and positive and negative dp/dt, between the control group and G-CSF group (**Table 1**). After reperfusion, however, G-CSF-treated hearts started to beat earlier than those of the control group (**Fig. 5a**). At 120 min after reperfusion, contractile function (LVDP) of G-CSF-treated hearts was significantly better than that of control hearts (**Fig. 5a**). Likewise, diastolic function (LVEDP) of G-CSF-treated hearts was better than that of control hearts (**Fig. 5a**). After ischemia-reperfusion, there was more viable myocardium (red lesion) in G-CSF-treated hearts than control hearts (**Fig. 5b**). The size of the infarct (white lesion) was significantly smaller in G-CSF-treated hearts than in control hearts (**Fig. 5b**).

Table 1 Basal hemodynamic parameters

	Control ($n = 7$)	G-CSF ($n = 7$)
HR (b.p.m.)	326 ± 34	334 ± 24
LVP (mmHg)	121.8 ± 24	117.3 ± 32
LVEDP (mmHg)	4.3 ± 1.3	4.5 ± 1.6
$+dp/dt$ (mmHg/s)	7,554 ± 643	7,657 ± 377
$-dp/dt$ (mmHg/s)	6,504 ± 638	6,670 ± 602

HR, heart rate; b.p.m., beats per minute; LVP, left ventricular pressure; LVEDP, left ventricular end-diastolic pressure; $+dp/dt$ and $-dp/dt$, positive and negative first derivatives for maximal rates of left ventricular pressure development.

DISCUSSION

In the present study, G-CSFR was found to be expressed on cardiomyocytes and cardiac fibroblasts, and G-CSF activated Jak2 and the downstream signaling molecule Stat3 in cultured cardiomyocytes. Treatment with G-CSF protected cultured cardiomyocytes from apoptotic cell death possibly through upregulation of Bcl-2 and Bcl-xL expression, suggesting that G-CSF has direct protective effects on cardiomyocytes through G-CSFR and the Jak-Stat pathway. This idea is further supported by the *in vivo* experiments. G-CSF enhanced Stat3 activity and increased expression of Bcl-2 and Bcl-xL in the infarcted heart where G-CSFR was markedly upregulated, thereby preventing cardiomyocyte apoptosis and cardiac dysfunction. These effects of G-CSF were abolished when Stat3 activation was disrupted in cardiomyocytes, suggesting that a direct action of G-CSF on cardiomyocytes has a crucial role in preventing left ventricular remodeling after myocardial infarction. Because noncardiomyocytes also expressed G-CSFR, the possibility exists that activation of G-CSF receptors on these cells modulates the beneficial effects of G-CSF on infarcted hearts.

The mobilization of bone marrow stem cells (BMSC) to the myocardium has been considered to be the main mechanism by which G-CSF ameliorates cardiac remodeling after myocardial infarction[1,6–8]. In this study, we showed that G-CSF reduces apoptotic cell death and effectively protects the infarcted heart, which is dependent on its direct action on cardiomyocytes through the Stat3 pathway. This antiapoptotic mechanism seems to be more important than induction of BMSC mobilization, because disruption of

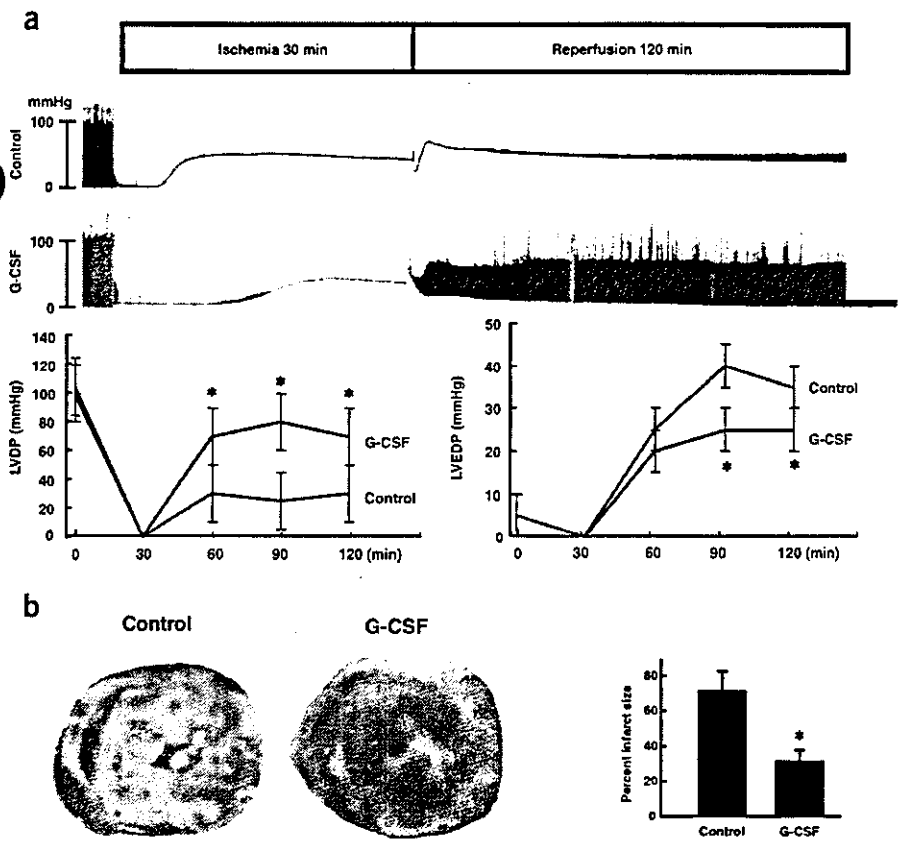

Figure 5 Direct effects of G-CSF on cardiac function after ischemia-reperfusion injury. (a) Representative left ventricular pressure records of control and G-CSF-treated hearts are shown (upper panel). The graphs show changes in LVDP (left) and LVEDP (right) during ischemia-reperfusion. $^*P < 0.05$ versus control hearts ($n = 7$). (b) The photographs show representative TTC staining of control hearts (Control) and G-CSF-treated hearts (G-CSF) after ischemia-reperfusion. The graph indicates myocardial infarct sizes for control hearts (Control) and G-CSF-treated hearts (G-CSF). Infarct sizes were calculated as described in **Supplementary Methods** online. $^*P < 0.05$ versus control hearts ($n = 7$).

this pathway by expressing dnStat3 in cardiomyocytes almost abolished the protective effects of G-CSF on cardiac remodeling after myocardial infarction. In addition, there was no difference in the effects of G-CSF on mobilization and cardiac homing of bone marrow cells, expansion of cardiac stem cells, and proliferation of cardiomyocytes between wild-type and dnStat3-Tg mice. The beneficial effects of G-CSF and stem cell factor on the infarcted heart has been described, but no evidence indicating that G-CSF induced cardiac homing of bone marrow cells in the infarcted heart has been shown[1]. In this study, we found favorable effects of G-CSF on the infarcted heart as early as 1 week after the treatment even though cardiac homing of bone marrow cells was not increased. Thus, we conclude that increased cardiac homing of bone marrow cells cannot account for improved function of the infarcted heart after G-CSF treatment.

The JAK-STAT pathway has been shown to induce various angiogenic factors besides antiapoptotic proteins[20,21]. The number of endothelial cells in the border zone was increased by G-CSF through Stat3 activation in cardiomyocytes. Consistent with this, we noted that G-CSF induces cardiac expression of angiogenic factors *in vitro* and *in vivo*, which appears to be mediated by cardiac Stat3 activation (M.H., Y.Q., H.T., T.M. & I.K., unpublished data). Moreover, we observed that the majority of apoptotic cells in the infarcted hearts was endothelial cells and that endothelial apoptosis was significantly inhibited by G-CSF treatment in wild-type mice but not in dnStat3-Tg mice (**Fig. 4a** and M.H., T.M. & I.K., unpublished data). Thus, activation of this pathway in cardiomyocytes by G-CSF may also promote angiogenesis and protect against endothelial apoptosis by producing angiogenic factors, resulting in the further prevention of cell death of cardiomyocytes and cardiac remodeling after myocardial infarction. The results in this study provide new mechanistic insights of the G-CSF therapy on infarcted hearts.

METHODS

For further details, please see **Supplementary Methods** online.

Cell culture. Cardiomyocytes prepared from ventricles of 1-d-old Wistar rats[27] were plated onto 60-mm plastic culture dishes at a concentration of 1×10^5 cells/cm^2 and cultured in Dulbecco modified Eagle medium (DMEM) supplemented with 10% fetal bovine serum (FBS) at 37 °C in a mixture of 95% air and 5% CO_2. The culture medium was changed to serum-free DMEM 24 h before stimulation. Generation and infection of recombinant adenovirus were performed as described[28].

Percoll enrichment of adult mouse cardiomyocytes and noncardiomyocytes. Adult mouse cardiomyocytes were prepared from 10-week-old C57BL/6 male mice according to the Alliance for Cellular Signaling protocol. We also prepared cardiomyocytes and noncardiomyocytes from myocardial infarction-operated or sham-operated C57BL/6 male mice. After digestion, cells were dissociated, resuspended in differentiation medium and loaded onto a discontinuous Percoll gradient. Cardiomyocytes or noncardiomyocytes were separately collected as described previously[29] and subsequently washed with 1 × phosphate-buffered saline for RT-PCR.

RNA extraction and RT-PCR analysis. Total RNA from adult mice cardiomyocytes was isolated by the guanidinium thiocyanate-phenol chloroform method. A total of 4 μg RNA was transcribed with MMLV reverse transcriptase and random hexamers. The cDNA was amplified using a mouse *Csf3r* exon 15 forward primer (5′-GTACTCTTGTCCACTACCTGT -3′) and an exon 17 reverse primer (5′-CAAGATACAAGGACCCCCAA -3′). We performed PCR under the following conditions: an initial denaturation at 94 °C for 2 min followed by a cycle of denaturation at 94 °C for 1 min, annealing at 58 °C for 1 min and extension at 72 °C for 1 min. We subjected samples to 40 cycles followed by a final extension at 72 °C for 3 min. The products were analyzed on a 1.5% ethidium bromide stained agarose gel.

Immunocytochemistry. Cardiomyocytes or noncardiomyocytes of neonatal rats cultured on glass cover slips were incubated with or without the antibody to G-CSFR (Santa Cruz Biotechnology) for 1 h, followed by incubation with Cy3-labeled secondary antibodies. After washing, we double-stained the cells with fluorescent phalloidin (Molecular Probes) for 1 h at room temperature.

Western blots. Western blot analysis was performed as described[5]. We probed the membranes with antibodies to phospho-Jak2, phospho-Stat3 (Cell Signaling), phospho-Jak1, phospho-Tyk2, phospho-Stat1, phospho-Stat5, anti-Jak1, Jak2, Tyk2, Stat1, Stat3, Stat5, Bcl-2, Bax, G-CSFR (Santa Cruz Biotechnology), Bcl-xL, Bad (Transduction Laboratories) or actin (Sigma-Aldrich). We used the ECL system (Amersham Biosciences Corp) for detection.

Animals and surgical procedures. Generation and genotyping of dnStat3-Tg mice have been previously described[28]. All mice used in this study were 8–10-week-old males, unless indicated. All experimental procedures were performed according to the guidelines established by Chiba University for experiments in animals and all protocols were approved by our institutional review board. We anesthetized mice by intraperitoneally injecting a mixture of 100 mg/kg ketamine and 5 mg/kg xylazine. Myocardial infarction was produced by ligation of the left anterior descending artery. We operated on dnStat3-Tg mice to induce myocardial infarction and randomly divided them into two groups, the G-CSF-treated group (10–100 μg/kg/d subcutaneously for 5 d consecutively, Kyowa Hakko Kogyo Co.) and the saline-treated group. We operated on nontransgenic mice as control groups using the same procedures and divided them into a G-CSF-treated group and a saline-treated group. Some mice were randomly chosen to be analyzed for initial area at risk by injection of Evans blue dye after producing myocardial infarction. There was no difference in initial area sizes at risk between saline-treated control and G-CSF-treated mice ($n = 5$; **Supplementary Fig. 11** online). We also determined initial infarct size by triphenyltetrazolium chloride staining on day 3. There was no significant difference in initial infarct size between saline-treated control and G-CSF-treated mice ($n = 5$; **Supplementary Fig. 12** online).

Echocardiography and catheterization. Transthoracic echocardiography was performed with an Agilent Sonos 4500 (Agilent Technology Co.) provided with an 11-MHz imaging transducer. For catheterization analysis, the right carotid artery was cannulated under anesthesia by the micro pressure transducers with an outer diameter of 0.42 mm (Samba 3000; Samba Sensors AB), which was then advanced into the left ventricle. Pressure signals were recorded using a MacLab 3.6/s data acquisition system (AD Instruments) with a sampling rate of 2,000 Hz. Mice were anesthetized as described above, and heart rate was kept at approximately 270–300 beats per minute to minimize data deviation when we measured cardiac function.

Histology. Hearts fixed in 10% formalin were embedded in paraffin, sectioned at 4 μm thickness, and stained with Masson trichrome. The extent of fibrosis was measured in three sections from each heart and the value was expressed as the ratio of Masson trichrome stained area to total left ventricular free wall. For apoptosis analysis, infarcted hearts were frozen in cryomolds, sectioned, and TUNEL labeling was performed according to the manufacturer's protocol (*In Situ* Apoptosis Detection kit; Takara) in combination with immunostainings for appropriate cell markers. Digital photographs were taken at magnification ×400, and 25 random high-power fields (HPF) from each heart sample were chosen and quantified in a blinded manner. We examined vascularization by measuring the number of capillary endothelial cells in light-microscopic sections taken from the border zone of the hearts 2 weeks after myocardial infarction. Capillary endothelial cells were identified by immunohistochemical staining with antibody to platelet endothelial cell adhesion molecule (PECAM; Pharmingen). Ten random microscopic fields in the border zone were examined and the number of endothelial cells was expressed as the number of PECAM-positive cells/HPF (magnification, ×400).

Statistical analysis. Data are shown as mean ± s.e.m. Multiple group comparison was performed by one-way analysis of variance (ANOVA) followed by the Bonferroni procedure for comparison of means. Comparison between two groups were analyzed by the two-tailed Student's *t*-test or two-way ANOVA. Values of $P < 0.05$ were considered statistically significant.

URL. Alliance for Cellular Signaling Procedure Protocols
http://www.signaling-gateway.org/data/cgi-bin/Protocols.cgi?cat=0

Note: Supplementary information is available on the Nature Medicine website.

ACKNOWLEDGMENTS

The authors thank J. Robbins (Children's Hospital Research Foundation, Cincinnati, Ohio) for a fragment of the αMHC gene promoter, M. Tamagawa for the analysis of Langendorff-perfused model, Kirin Brewery Co., Ltd. for their kind gift of G-CSF, and M. Watanabe and E. Fujita for their technical assistance. This work was supported by a Grant-in-Aid for Scientific Research, Developmental Scientific Research, and Scientific Research on Priority Areas from the Ministry of Education, Science, Sports, and Culture and by the Program for Promotion of Fundamental Studies in Health Sciences of the Organization for Drug ADR Relief, R&D Promotion and Product Review of Japan (to I.K.) and Japan Research Foundation for Clinical Pharmacology (to T.M.).

COMPETING INTERESTS STATEMENTS

The authors declare that they have no competing financial interests.

Received 8 September 2004; accepted 19 January 2005
Published online at http://www.nature.com/naturemedicine/

1. Orlic, D. *et al.* Mobilized bone marrow cells repair the infarcted heart, improving function and survival. *Proc. Natl. Acad. Sci. USA* **98**, 10344–10349 (2001).
2. Ohtsuka, M. *et al.* Cytokine therapy prevents left ventricular remodeling and dysfunction after myocardial infarction through neovascularization. *FASEB J.* **18**, 851–853 (2004).
3. Moon, C. *et al.* Erythropoietin reduces myocardial infarction and left ventricular functional decline after coronary artery ligation in rats. *Proc. Natl. Acad. Sci. USA* **100**, 11612–11617 (2003).
4. Parsa, C.J. *et al.* A novel protective effect of erythropoietin in the infarcted heart. *J. Clin. Invest.* **112**, 999–1007 (2003).
5. Zou, Y. *et al.* Leukemia inhibitory factor enhances survival of cardiomyocytes and induces regeneration of myocardium after myocardial infarction. *Circulation* **108**, 748–753 (2003).
6. Minatoguchi, S. *et al.* Acceleration of the healing process and myocardial regeneration may be important as a mechanism of improvement of cardiac function and remodeling by postinfarction granulocyte colony-stimulating factor treatment. *Circulation* **109**, 2572–2580 (2004).
7. Adachi, Y. *et al.* G-CSF treatment increases side population cell infiltration after myocardial infarction in mice. *J. Mol. Cell. Cardiol.* **36**, 707–710 (2004).
8. Kawada, H. *et al.* Nonhematopoietic mesenchymal stem cells can be mobilized and differentiate into cardiomyocytes after myocardial infarction. *Blood* **104**, 3581–3587 (2004).
9. Avalos, B.R. Molecular analysis of the granulocyte colony-stimulating factor receptor. *Blood* **88**, 761–777 (1996).
10. Demetri, G.D. & Griffin, J.D. Granulocyte colony-stimulating factor and its receptor. *Blood* **78**, 2791–808 (1991).
11. Berliner, N. *et al.* Granulocyte colony-stimulating factor induction of normal human bone marrow progenitors results in neutrophil-specific gene expression. *Blood* **85**, 799–803 (1995).
12. Orlic, D. *et al.* Bone marrow cells regenerate infarcted myocardium. *Nature* **410**, 701–705 (2001).
13. Asahara, T. *et al.* Bone marrow origin of endothelial progenitor cells responsible for postnatal vasculogenesis in physiological and pathological neovascularization. *Circ. Res.* **85**, 221–228 (1999).
14. Kocher, A.A. *et al.* Neovascularization of ischemic myocardium by human bone-marrow-derived angioblasts prevents cardiomyocyte apoptosis, reduces remodeling and improves cardiac function. *Nat. Med.* **7**, 430–436 (2001).
15. Jackson, K.A. *et al.* Regeneration of ischemic cardiac muscle and vascular endothelium by adult stem cells. *J. Clin. Invest.* **107**, 1395–1402 (2001).
16. Balsam, L.B. *et al.* Haematopoietic stem cells adopt mature haematopoietic fates in ischaemic myocardium. *Nature* **428**, 668–673 (2004).
17. Murry, C.E. *et al.* Haematopoietic stem cells do not transdifferentiate into cardiac myocytes in myocardial infarcts. *Nature* **428**, 664–668 (2004).
18. Norol, F. *et al.* Influence of mobilized stem cells on myocardial infarct repair in a nonhuman primate model. *Blood* **102**, 4361–4368 (2003).
19. Aarts, L.H., Roovers, O., Ward, A.C. & Touw, I.P. Receptor activation and 2 distinct COOH-terminal motifs control G-CSF receptor distribution and internalization kinetics. *Blood* **103**, 571–579 (2004).
20. Benekli, M., Baer, M.R., Baumann, H. & Wetzler, M. Signal transducer and activator of transcription proteins in leukemias. *Blood* **101**, 2940–2954 (2003).
21. Smithgall, T.E. *et al.* Control of myeloid differentiation and survival by Stats. *Oncogene* **19**, 2612–2618 (2000).
22. Dumont, E.A. *et al.* Cardiomyocyte death induced by myocardial ischemia and reperfusion: measurement with recombinant human annexin-V in a mouse model. *Circulation* **102**, 1564–1568 (2000).
23. van Heerde, W.L. *et al.* Markers of apoptosis in cardiovascular tissues: focus on Annexin V. *Cardiovasc. Res.* **45**, 549–559 (2000).
24. Bromberg, J. Stat proteins and oncogenesis. *J. Clin. Invest.* **109**, 1139–1142 (2002).
25. El-Adawi, H. *et al.* The functional role of the JAK-STAT pathway in post-infarction remodeling. *Cardiovasc. Res.* **57**, 129–138 (2003).
26. Matsuura, K. *et al.* Adult cardiac Sca-1-positive cells differentiate into beating cardiomyocytes. *J. Biol. Chem.* **279**, 11384–11391 (2004).
27. Zou, Y. *et al.* Both Gs and Gi proteins are critically involved in isoproterenol-induced cardiomyocyte hypertrophy. *J. Biol. Chem.* **274**, 9760–9770 (1999).
28. Funamoto, M. *et al.* Signal transducer and activator of transcription 3 is required for glycoprotein 130-mediated induction of vascular endothelial growth factor in cardiac myocytes. *J. Biol. Chem.* **275**, 10561–10566 (2000).
29. Ikeda, K. *et al.* The effects of sarpogrelate on cardiomyocyte hypertrophy. *Life Sci.* **67**, 2991–2996 (2000).

Cell Tissue Res (2004) 316:141–153
DOI 10.1007/s00441-004-0862-1

REGULAR ARTICLE

Kohei Tsuchiya · Taisuke Mori · Guoping Chen · Takashi Ushida · Tetsuya Tateishi · Takeo Matsuno · Michiie Sakamoto · Akihiro Umezawa

Custom-shaping system for bone regeneration by seeding marrow stromal cells onto a web-like biodegradable hybrid sheet

Received: 28 August 2003 / Accepted: 23 January 2004 / Published online: 4 March 2004

Abstract New bone for the repair or the restoration of the function of traumatized, damaged, or lost bone is a major clinical need, and bone tissue engineering has been heralded as an alternative strategy for regenerating bone. A novel web-like structured biodegradable hybrid sheet has been developed for bone tissue engineering by preparing knitted poly(DL-lactic-*co*-glycolic acid) sheets (PLGA sheets) with collagen microsponges in their openings. The PLGA skeleton facilitates the formation of the hybrid sheets into desired shapes, and the collagen microsponges in the pores of the PLGA sheet promote cell adhesion and uniform cell distribution throughout the sheet. A large number of osteoblasts established from marrow stroma adhere to the scaffolds and generate the desired-shaped bone in combination with these novel sheets. These results indicate that the web-like structured novel sheet shows promise for use as a tool for custom-shaped bone regeneration in basic research on osteogenesis and for the development of therapeutic applications.

Keywords Bone regeneration · Tissue engineering · Scaffold · Marrow stroma · Polymer · KUSA-A1 cells

This work was supported in part by a grant from the Ministry of Education, Culture, Sports, Science, and Technology of Japan, Health and Labour Sciences Research Grants (translational research), and the Organization for Pharmaceutical Safety and Research (to A.U.)

K. Tsuchiya · T. Mori · A. Umezawa (✉)
Department of Reproductive Biology and Pathology,
National Research Institute for Child and Health Development,
Okura, Setagaya, 157-8535 Tokyo, Japan
e-mail: umezawa@1985.jukuin.keio.ac.jp

K. Tsuchiya · T. Mori · M. Sakamoto
Department of Pathology,
Keio University School of Medicine,
160-8582 Tokyo, Japan

K. Tsuchiya · T. Matsuno
Department of Orthopedic Surgery,
Asahikawa Medical College,
078-8802 Hokkaido, Japan

K. Tsuchiya · G. Chen · T. Tateishi
Biomaterials Center,
National Institute for Materials Science,
305-0044 Ibaraki, Japan

G. Chen · T. Ushida
Tissue Engineering Research Center,
National Institute of Advanced Industrial Science and Technology,
661-0974 Hyogo, Japan

T. Ushida
Center for Disease Biology and Integrative Medicine,
School of Medicine, University of Tokyo,
113-0033 Tokyo, Japan

Introduction

New bone for the replacement or restoration of the function of traumatized, damaged, or lost bone is a major clinical and socioeconomic need. Bone formation strategies, although attractive, have yet to yield functional and mechanically competent bone. Autografts (bone obtained from another site in the same subject of the same species) are currently the gold standard for bone repair and substitution, but the use of autografts has several serious disadvantages, such as additional expense and trauma to the patient, the possibility of donor-site morbidity, and limited availability (Glowacki and Mulliken 1985; Bauer and Muschler 2000). Because of these problems, bone tissue engineering has been heralded as an alternative strategy for the regeneration of bone (Langer and Vacanti 1993; Crane et al. 1995; Boyan et al. 1999).

Bone has a highly organized structure composed of a calcified connective tissue matrix formed by the proliferation and differentiation of osteoprogenitors into mature osteoblasts (Maniatopoulos et al. 1988; Pitaru et al. 1993). The osteoblasts belong to the stromal fibroblastic system of the bone marrow, which contains other stromal cells, such as chondrocytes and myoblasts (Friedenstein 1976; Owen and Friedenstein 1988; Haynesworth et al. 1992). We have shown that mouse stromal cells are able to differentiate into cardiomyocytes (Makino et al. 1999;

Gojo et al. 2003), endothelial cells, neuronal cells (Kohyama et al. 2001), and adipocytes (Umezawa et al. 1991). We have previously established a murine osteoblast cell line, KUSA-A1, and shown that clonal stromal cells can generate bone in vivo (Umezawa et al. 1992). Marrow stromal cells are expected to serve as a good source for cell therapy, in addition to embryonic stem cells and fetal cells. Although these precursor cells have been reported to be stem cells, it remains unknown as to whether they are homogeneous or whether they constitute subpopulations of cells committed to various lineages of differentiation (Owen and Friedenstein 1988). The acquisition of a large number of osteoblast precursors as a cell source and the control of differentiation are essential to the success of the production of tissue-engineered bone for clinical application (Minuth et al. 1998).

Temporary three-dimensional scaffolds play an important role in the manipulation of the functions of osteoblasts (Chicurel et al. 1998) and in the guidance of the formation of new bones into the desired shapes (Ishaug et al. 1997; Ishaug-Riley et al. 1998), in the bone tissue-engineering approach. These scaffolds should be biocompatible, osteoconductive, biodegradable, highly porous with a large surface-to-volume ratio, mechanically strong, and malleable into the desired shapes. Synthetic polymers, such as poly(lactic acid), poly(glycolic acid), and poly(DL-lactic-*co*-glycolic acid), which is abbreviated here as PLGA, are easily processed into the desired shapes and are mechanically strong (Langer and Vacanti 1993; Ishaug et al. 1997; Ishaug-Riley et al. 1998; Mikos et al. 1998). Moreover, their degradation time can be manipulated by controlling their crystallinity, molecular weight, and the ratio of lactic acid to glycolic acid copolymer (Thomson et al. 1995). Collagen is the primary component of extracellular bone matrix and has been demonstrated to produce good osteoconductivity (Aronow et al. 1990). Synthetic polymers, on the other hand, lack cell recognition signals, and their hydrophobic properties hinder the uniform seeding of cells in three dimensions. However, since collagen scaffolds are mechanically weak, these materials have been hybridized to combine their advantages and provide excellent three-dimensional porous biomaterials for bone tissue engineering.

We have developed collagen-hybridized PLGA sponge and have reported good biocompatibility both for cartilage tissue engineering with mature bovine chondrocytes (Sato et al. 2001; Chen et al. 2003) and for bone tissue engineering with osteoblasts isolated from marrow cells (Ochi et al. 2003). The sponges organize satisfactory cartilage and bone tissue when the cells fill the pores of the scaffold. The uniform distribution of the cells throughout the scaffolds is imperative for the development of homogeneous tissue, but special seeding techniques, such as stir flask culture or perfusion bioreactor culture, are required to produce an even distribution reliably (Vunjak-Novakovic et al. 1998; Freed et al. 1999). Since simple static seeding methods tend to produce an uneven distribution with large patches of cells on the surface, we have hybridized collagen microsponges with PLGA sheets. The sheets have a collagen fiber network in the openings of the PLGA fiber sheets. The findings that the sheets trap cells, that they can be laminated or rolled to control their shape for tissue engineering, and that they also have the capacity to supply minerals by depositing apatite particulates on the surface of collagen microsponges indicate their great advantages. In this study, we have shown that, when the novel web-like structured sheets are used as a scaffold for bone tissue engineering, an even cell distribution and the control of its shape can be achieved.

Materials and methods

Scaffold fabrication

The hybrid sheet was prepared by allowing collagen microsponges to form in the openings of PLGA knitted sheets as previously described (Chen et al. 2003). Briefly, as shown in Fig. 1A, a knitted Vicryl sheet made of polylactin 910 (a 90:10 co-polymer of glycolic acid and lactic acid) was immersed in a type I bovine collagen acidic solution (pH 3.2, 0.5% by weight, Koken, Tokyo, Japan) and frozen at −80°C for 12 h. It was then freeze-dried under vacuum (0.2 Torr) for 24 h to allow the formation of collagen microsponges. The collagen microsponges were further cross-linked by treatment with glutaraldehyde vapor saturated with a 25% aqueous glutaraldehyde solution at 37°C for 4 h. After the cross-linking, the sponge was treated with a 0.1 M aqueous glycine solution to block unreacted aldehyde groups. After being washed with deionized water and freeze-dried, the collagen-hybridized PLGA (PLGA/COL) sheet was complete. The sheets were sterilized with ethylene oxide for cell culture.

Cell culture

KUSA-A1 cells were cultured as described previously (Umezawa et al. 1992; Kohyama et al. 2001; Ochi et al. 2003).

Cell seeding of a PLGA/COL sheet

A PLGA/COL sheet was placed into a 100-mm culture dish (Falcon) and covered with a silicone rubber framework. A 2-ml volume of KUSA-A1 cell suspension at a density of 5×10^6/ml was dropped onto the PLGA/COL sheet (area: 4 cm^2). After cultivation for 6 h, the sheet was turned over and re-seeded with the same number of cells on the reverse side. For comparison, a KUSA-A1 suspension (1×10^7 cells/ml) was injected into collagen hybrid PLGA sponges, and the injected sponges were incubated at 37°C for more than 30 min. The sponges were then transplanted into the subcutaneous tissue of C3H mice as previously described (Ochi et al. 2003).

Scanning electron microscopy

PLGA sheets and PLGA/COL sheets were examined by scanning electron microscopy (SEM). They were cut into small pieces with scissors and coated with gold by means of a sputter coater (Sanyu Denshi, Tokyo, Japan; gas pressure: 50 mtorr, current: 5 mA, coating time: 180 s). The samples were examined with a JSM-6400Fs scanning electron microscope (JEOL, Tokyo, Japan) operated at a voltage of 3 kV.

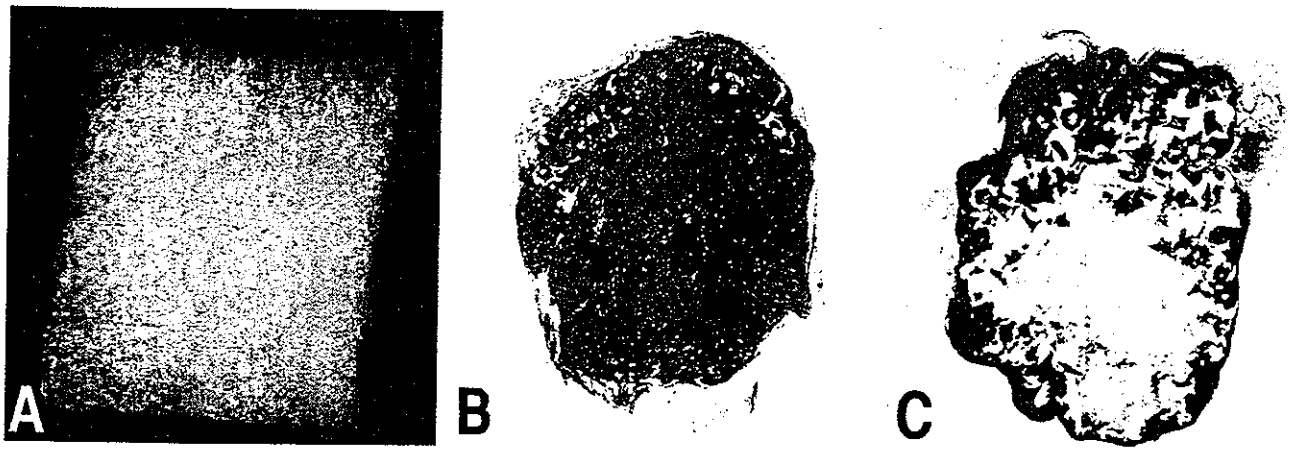

Fig. 1A–C Bone formation in collagen hybrid PLGA sponge. Macroscopic appearance of the collagen hybrid PLGA sponge (A). Complete bone formation of an in vivo 4-week construct based on KUSA-A1 cells and collagen hybrid PLGA sponge (B). Some constructs showed uneven bone distribution. Living cells did not completely fill the pore cavities of the sponge (C). ×5

Transmission electron microscopy

Samples cultured in vitro for 1 day and 2 weeks were examined by transmission electron microscopy (TEM). They were fixed in 2.5% glutaraldehyde, postfixed in 1% osmium tetroxide, dehydrated, and embedded in resin. Ultrathin sections (70–90 nm) were cut and stained with 2% uranyl acetate and Reynold's lead citrate before being examined with a JEM-1200 EX microscope (JOEL) at 80 kV.

In vivo assay

All animals received humane care in compliance with the "Principles of Laboratory Animal Care" formulated by the National Society for Medical Research and the "Guide for the Care and Use of Laboratory Animals" prepared by the Institute of Laboratory Animal Resources and published by the US National Institutes of Health (NIH Publication no. 86–23, revised 1985). The operation protocols were accepted by the Laboratory Animal Care and Use Committee of the National Research Institute for Child and Health Development (Tokyo) and by Keio University School of Medicine.

Laminated sheet implantation onto calvarial defects

Surgery was performed under anesthesia with Nembutal (50 mg/kg, i.p.). A midline skin incision approximately 1 cm long was made on the dorsal surface of the cranium, and the periosteum was removed. A 4.3-mm-diameter full-thickness circular defect was created in the skull with a trephine bar (Hasegawa Medical, Tokyo, Japan) attached to an electric handpiece, with minimal penetration of the dura. The defect was covered with three sheets of cell-loaded scaffolds cut to fit the shape of the defect. The scalp was then closed with 6-0 nylon sutures, and the animals were given access to food and allowed to behave *ad libitum*. Ten defects were left untreated, 10 defects were treated with PLGA/COL sheets alone as controls, and 10 defects were filled with PLGA/COL sheets seeded with KUSA-A1 cells.

Custom-shaped bone formation in mice

With the aim of producing long bone, cylinder-like bone was formed by rolling KUSA-A1-seeded sheets around a silicone rod 3 mm in diameter. The ends of the sheets were hemmed with 4-0 Vicryl dissolvable stitches. The rolled sheets were transplanted into subcutaneous tissue for 4 weeks, flat or after being knotted. Tissue-engineered phalanges were formed in a similar manner. KUSA-A1-seeded sheets were wrapped around a silicone rubber block trimmed in advance to the shape of the distal phalanx and transplanted into subcutaneous tissue. After cultivation in syngeneic C3H/He mice, NOD/SCID mice, and NOD/SCID/IL2-receptor γ knock-out immunodeficient mice (NOG), the specimens were extracted and examined histologically.

Histological and Immunohistochemical staining

Calvaria, femurs, and subcutaneous specimens were dissected at various times after implantation and fixed and decalcified for 1 week in 10% EDTA (pH 8.0) solution. After dehydration in ascending concentrations of ethanol and xylene, the transplants were embedded in paraffin and sectioned. The paraffin sections were then deparaffinized, hydrated, and either were stained with hematoxylin and eosin or were immunohistochemically stained with anti-human Factor VIII mAb (DAKO, Carpenteria, Calif.) to detect angiogenesis.

Results

Bone distribution of sponges

We previously reported that KUSA-A1 cells generated cuboidal bone when used in combination with PLGA/COL hybrid sponge. In those experiments, the KUSA-A1 cells were distributed evenly into sponges and had generated cuboidal bone in the subcutaneous tissue at 8 weeks (Fig. 1A, B); however, some of them exhibited uneven bone formation. The bone was generated mainly at the periphery of the sponge, like an eggshell (Fig. 1C).

Collagen-hybridized PLGA sheet

We developed the sheet-style scaffold to prevent uneven bone formation (Fig. 2A–C). The synthetic biodegradable polymer, PLGA, which was 200 μm thick, was hybridized with collagen microsponges. SEM analysis revealed that the collagen microsponges overlaid the interstices of the

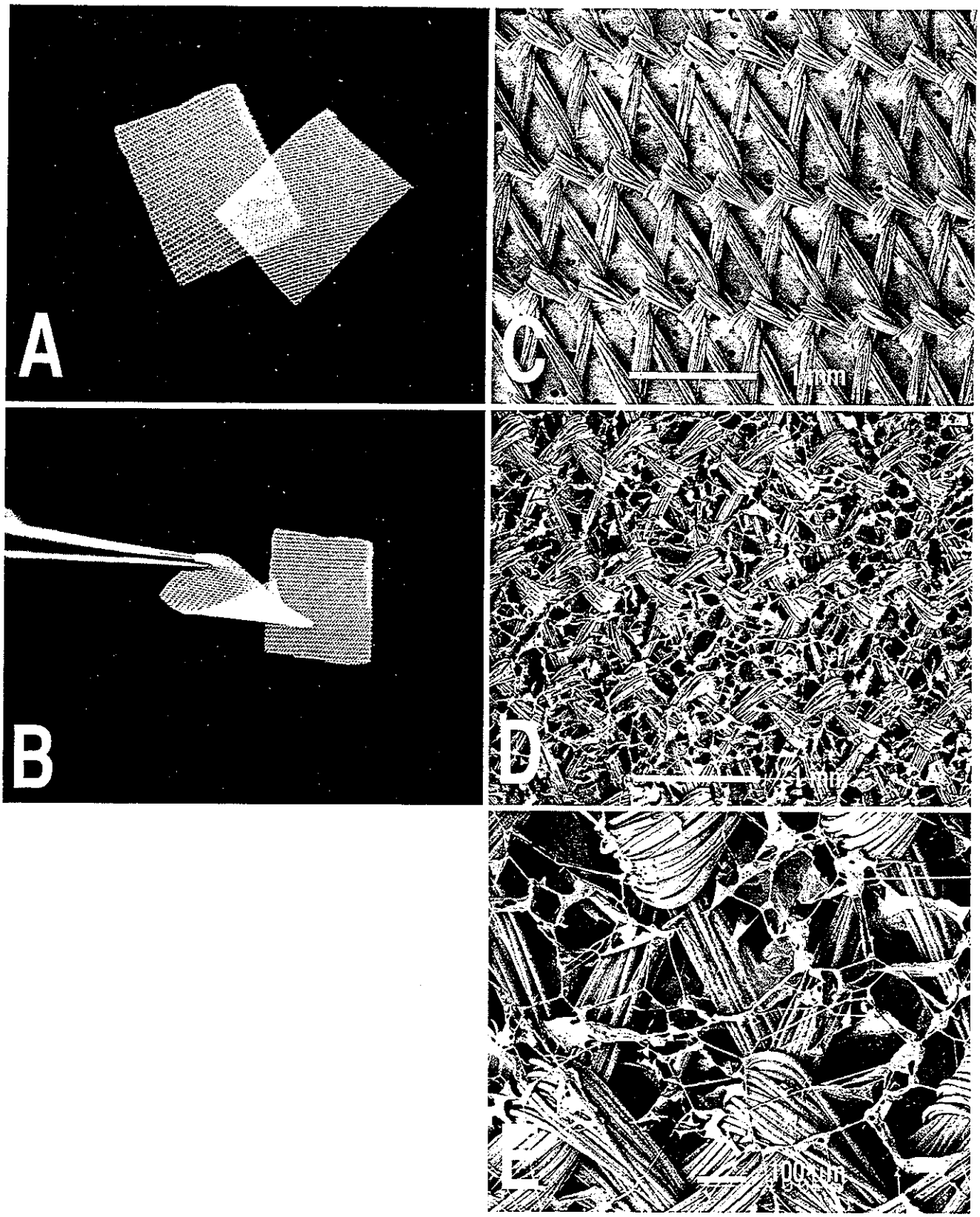

Fig. 2A–E Collagen hybrid PLGA sheet. The thin 200 µm sheets are easy to handle (**A, B**). SEM micrographs of a PLGA sheet without collagen (**C**) and a hybrid sheet with collagen (**D**). Higher magnification of the hybrid sheet (**E**)

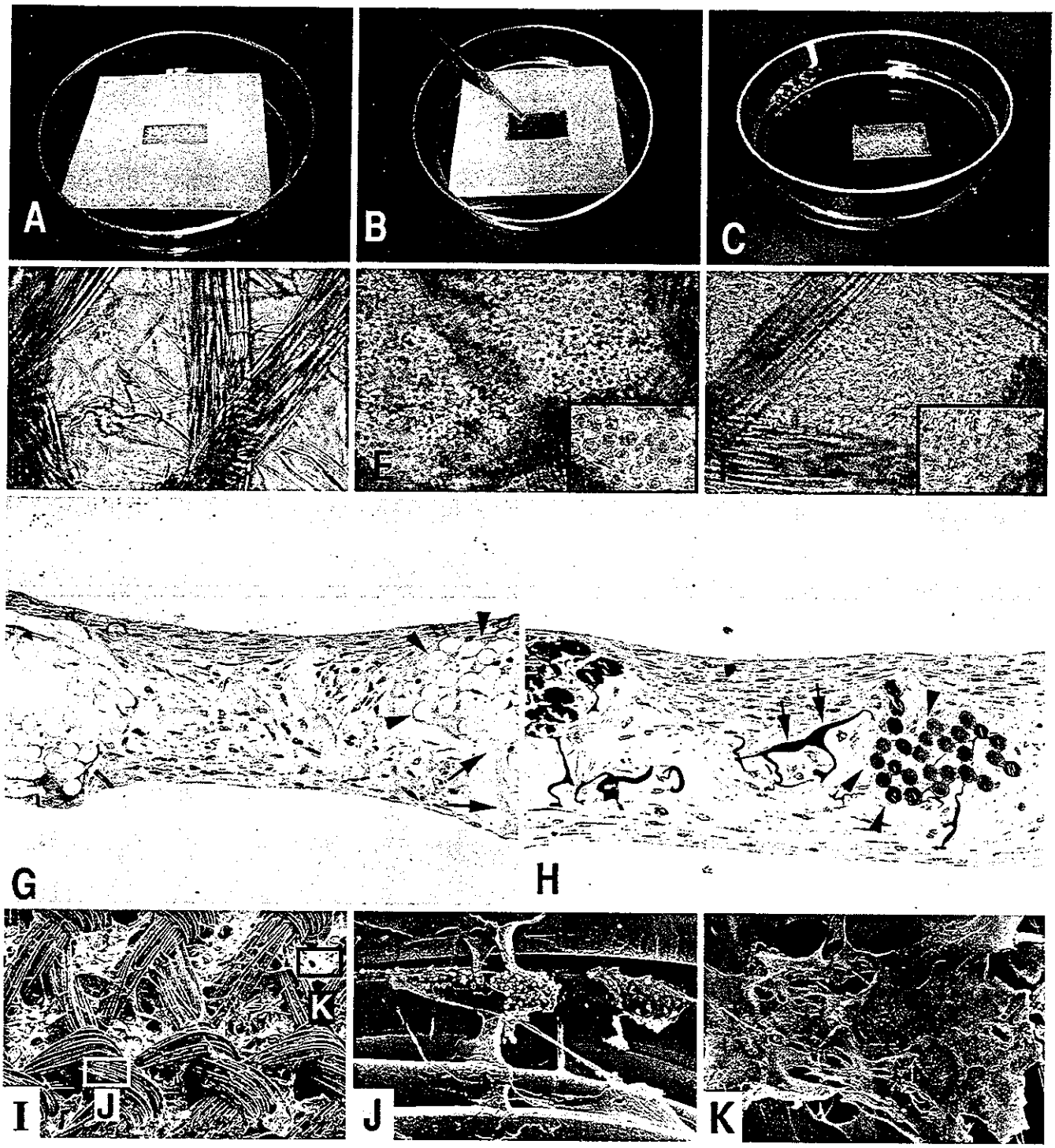

Fig. 3A–K Process of cell seeding. **A–C** Cell seeding of the sheet. The sheet was framed in silicone rubber (**A**), and the cell suspension was simply dropped onto the sheet (**B**). The silicone rubber was removed 6 h after seeding, and the sheet was cultured in growth medium (**C**). **D–F** Phase-contrast micrographs of a cell-seeded sheet. The openings of the PLGA/COL sheet (**D**) were filled with cells at 30 min (**E**) and were completely covered with abundant extracellular matrix at 1 week (**F**). **G, H** Toluidine-blue stained cross sections of the cell-seeded sheet at 1 day (**G**) and 2 weeks (**H**). The thickness of the sheet had increased (*arrowheads* PLGA fibers, *arrows* collagen fibers). **I–K** SEM micrographs of a PLGA/COL sheet after cell seeding. A portion of PLGA fiber (**J**) and collagen microsponge (**K**) are shown. **D–F** ×200, **G, H** ×400, **I** ×50, **J, K** ×200

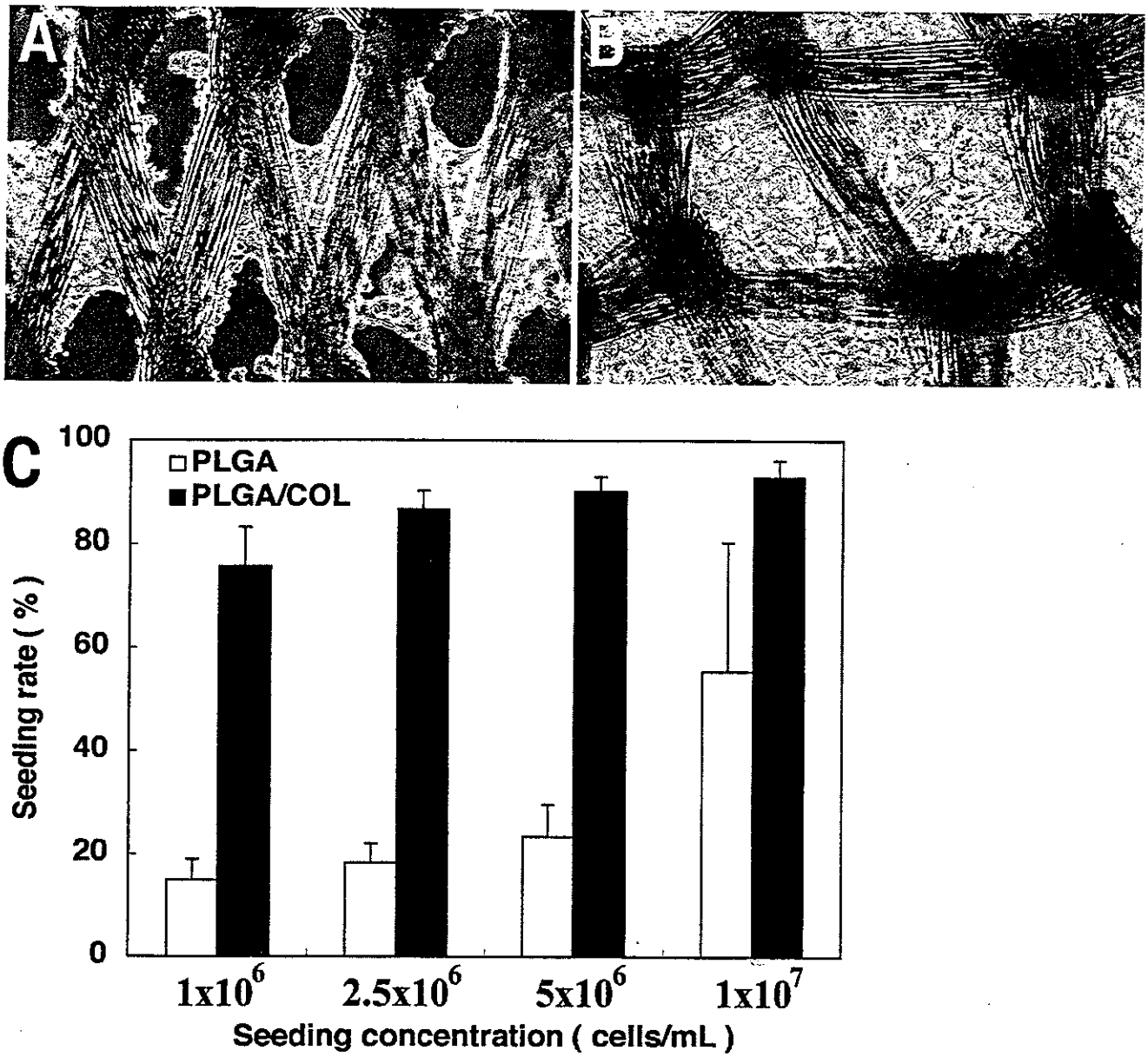

Fig. 4A–C Effect of collagen microsponges on cell adhesion. Microscopic appearance of a PLGA sheet (**A**) and PLGA/COL (**B**) sheet 1 day after seeding the same number of cells in suspension (1×10^7 cells). The seeding rates (**C**) indicate the differences in the number of adhering cells between the two sheets at the initial cell seeding concentrations. **A, B** ×100

fabricated web-like PLGA sheets (Fig. 2D, E). This structure was expected to entrap a large number of cells.

Cells uniformly trapped in sheets with a web-like pattern

A cell suspension was simply dropped onto the sheets (Fig. 3A–C), and the collagen microsponges had filled with precipitated cells 30 min after seeding. The cells had adhered completely at 3 h (Fig. 3D–F), whereas the non-hybridized PLGA sheets did not trap cells efficiently. The cells continued to spread and generate matrix over the sheets, so that at 2 weeks, the sheets were completely covered by extracellular matrix, and the thickness of sheet had increased (Fig. 3G, H). After in vitro culture for 1 day, SEM examination revealed the preference of cells for components of the scaffold (Fig. 3I–K). A large number of cells had adhered to the collagen microsponge portion rather than to the PLGA fibers. Since synthetic polymers lack cell recognition signals, and since their hydrophobic properties hinder cell adhesion, the hybridization of collagen microsponges was advantageous in achieving cell retention.

The PLGA/COL sheets trapped significantly more cells than non-hybridized control PLGA sheets (Fig. 4A, B). The numbers of cells that had adhered to the sheets at 6 h after seeding increased with the initial cell seeding concentration (Fig. 4C).